AD-A050 494 DAVID W TAYLOR NAVAL SHIP RESEARCH AND DEVELOPMENT CE--ETC F/G 13/11
THE EFFECTS OF CAM AND NOZZLE CONFIGURATIONS ON THE PERFORMANCE--ETC(U)
NOV 77 K R READER

UNCLASSIFIED DTNSRDC/ASED-393 NL

| OF |
AD
A050494

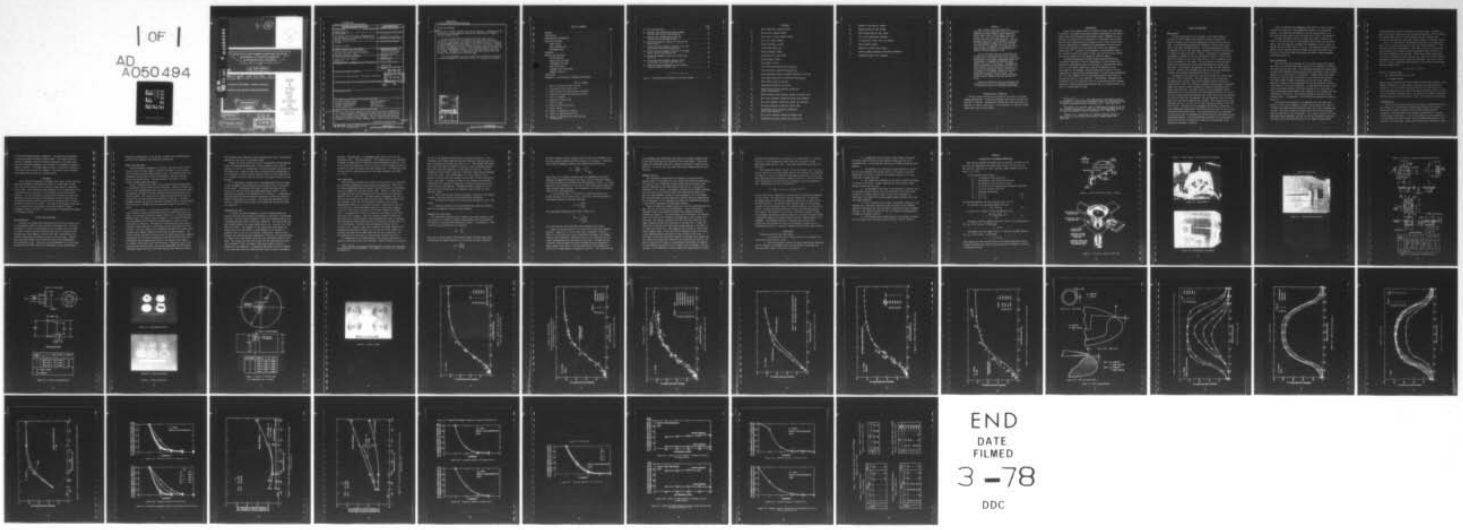

END
DATE
FILMED
3-78
DDC

12

DEPARTMENT OF THE NAVY
DTNSRDC

THE EFFECTS OF CAM AND NOZZLE CONFIGURATIONS ON THE PERFORMANCE OF A CIRCULATION CONTROL ROTOR PNEUMATIC VALVING SYSTEM

by

Kenneth R. Reader

Final rept. Oct 73 - Jan 74,

Approved for Public Release: Distribution Unlimited

AVIATION AND SURFACE EFFECTS DEPARTMENT

DTNSRDC/ASED-393

Nov 77

49 p.

F41421

F41421200

DAVID W. TAYLOR NAVAL SHIP RESEARCH AND DEVELOPMENT CENTER

BETHESDA, MARYLAND 20084

UNCLASSIFIED

SECURITY CLASSIFICATION OF THIS PAGE (When Data Entered)

REPORT DOCUMENTATION PAGE		READ INSTRUCTIONS BEFORE COMPLETING FORM
1. REPORT NUMBER DTNSRDC ASED-393	2. GOVT ACCESSION NO.	3. RECIPIENT'S CATALOG NUMBER
4. TITLE (and Subtitle) THE EFFECTS OF CAM AND NOZZLE CONFIGURATION ON THE PERFORMANCE OF A CIRCULATION CONTROL ROTOR PNEUMATIC VALVING SYSTEM		5. TYPE OF REPORT & PERIOD COVERED Final Oct 73 - Jan 74 6. PERFORMING ORG. REPORT NUMBER
7. AUTHOR(s) Kenneth R. Reader		8. CONTRACT OR GRANT NUMBER(s)
9. PERFORMING ORGANIZATION NAME AND ADDRESS David W. Taylor Naval Ship R&D Center Aviation and Surface Effects Department Bethesda, Maryland 20084		10. PROGRAM ELEMENT, PROJECT, TASK AREA & WORK UNIT NUMBERS Program Element 62241N Task Area F41.421.200 Work Unit 1690-100
11. CONTROLLING OFFICE NAME AND ADDRESS Naval Air Systems Command NAVAIR 320 Washington, D.C. 20361		12. REPORT DATE November 1977 13. NUMBER OF PAGES 49
14. MONITORING AGENCY NAME & ADDRESS(if different from Controlling Office)		15. SECURITY CLASS. (of this report) UNCLASSIFIED 15a. DECLASSIFICATION/DOWNGRADING SCHEDULE

16. DISTRIBUTION STATEMENT (of this Report)

Approved for Public Release: Distribution Unlimited

17. DISTRIBUTION STATEMENT (of the abstract entered in Block 20, if different from Report)

18. SUPPLEMENTARY NOTES

19. KEY WORDS (Continue on reverse side if necessary and identify by block number)

Circulation Control Rotor	Mass Flow Modulation
Pneumatic Valving System	Nozzles Effects
Cam-Type Valving System	Cam Effects
Pressure Modulation	Exit Area Effects

20. ABSTRACT (Continue on reverse side if necessary and identify by block number)

Basic research was conducted on the sensitivity of such component parts of a cam-type pneumatic valving system as cam eccentricity, nozzle aspect ratio, nozzle shape, nozzle endplates, slot exit area, and transition zone between the nozzle and blade entrance. Data are presented which show how systematic variations of these components affect the total pressure loss

(Continued on reverse side)

DD FORM 1 JAN 73 1473 EDITION OF 1 NOV 65 IS OBSOLETE
S/N 0102-014-6601

UNCLASSIFIED
SECURITY CLASSIFICATION OF THIS PAGE (When Data Entered)

(Block 20 continued)

coefficient, the mass flow rate, and the jet velocity. Information on the sensitivity of these parameters enhances the capabilities to design a cam-type pneumatic valve.

It was concluded that cam eccentricity had no effect on the characteristic curve for total pressure loss coefficient versus area coefficient. Accordingly, no stringent requirement should be encountered in changing the cross-sectional shape or the size of the nozzle. Streamlining of the transition section between the nozzle and blade entrance did not affect the pressure recovery in the operational range of the valve nor the shape or the harmonic content of the loss coefficient or mass flow rate curves. The addition of endplates to the nozzle reduced the total pressure losses between the hub and the blade.

The area coefficient and total pressure loss coefficient are shown to be adequate parameters to correlate the data for different valve models.

TABLE OF CONTENTS

LIST OF FIGURES

NOTATION

A	Open nozzle area, square inches
A_c	Control area, square inches
A_o	Inlet area to blade, square inches
A_s	Slot area, square inches
C	Nozzle periphery, inches
C_A	Area coefficient A_c/A_s
d	Nozzle diameter, inches
e	Eccentricity of cam, inches
H	Nozzle height, inches
h	Slot height, inches
K	Loss coefficient defined by P_h-P_b/P_b-p_n
K_A	Loss coefficient defined by P_h-P_b/P_b-p_b
K_1	Loss coefficient based on dynamic pressure at the slot
K_R	Total gage pressure loss coefficient $P_B-p_\infty/P_H-P_\infty$
$\dot{m}$	Mass efflux, slugs per second
n	Conditions defined at the nozzle
P_B	Blade entrance total pressure, pounds per square inch absolute
P_b	Blade entrance total pressure, pounds per square inch
P_d	Duct total pressure, pounds per square foot absolute
P_H	Hub total pressure, pounds per square inch absolute
P_h	Hub total pressure, pounds per square inch
P_∞	Free-stream static pressure, pounds per square foot absolute
p_b	Duct static pressure, pounds per square inch
p_∞	Atmospheric pressure, pounds per square inch

R	Radius of cam contour, inches
R_o	Minimum radius of cam, inches
R_1	Mean eccentricity of cam, inches
T_d	Duct total temperature, degrees
V_j	Jet velocity at exit, feet per second
W	Nozzle width, inches
r	Radius of circular cam, inches
η_o	General lumped discharge coefficient parameter
ψ	Azimuthal angle of cam, degrees

ABSTRACT

Basic research was conducted on the sensitivity of such component parts of a cam-type pneumatic valving system as cam eccentricity, nozzle aspect ratio, nozzle shape, nozzle endplates, slot exit area, and transition zone between the nozzle and blade entrance. Data are presented which show how systematic variations of these components affects the total pressure loss coefficient, the mass flow rate, and the jet velocity. Information on the sensitivity of these parameters enhances the capabilities to design a cam-type pneumatic valve.

It was concluded that cam eccentricity had no effect on the characteristic curve for total pressure loss coefficient versus area coefficient. Accordingly, no stringent requirement should be encountered in changing the cross-sectional shape or the size of the nozzle. Streamlining of the transition section between the nozzle and blade entrance did not affect the pressure recovery in the operational range of the valve nor the shape or the harmonic content of the loss coefficient or mass flow rate curves. The addition of endplates to the nozzle reduced the total pressure losses between the hub and the blade.

The area coefficient and total pressure loss coefficient are shown to be adequate parameters to correlate the data for different valve models.

ADMINISTRATIVE INFORMATION

The work reported herein was sponsored by the Naval Air Systems Command (NAVAIR-320). Funding was provided under Project F41.421.210, Work Unit 1-1690-100. Measurements reported here were taken prior to adoption of a metric unit policy. In the interest of time and economy, metric units have not been added.

INTRODUCTION

As part of an ongoing effort to provide a better, more efficient helicopter, the Aviation and Surface Effects Department of the David W. Taylor Naval Ship Research and Development Center (DTNSRDC) has been applying circulation control aerodynamics to helicopter rotor models. The successful application of circulation control (CC) to helicopters has been demonstrated at DTNSRDC by the development of two CC rotor models which exhibited control simplicity as well as competitive efficiencies.[1,2] A typical rotor geometry is illustrated in Figure 1 for a single slotted "low speed" concept, and the circulation control hub used in previous CC rotor models is shown in Figure 2.

Although the pneumatic valving system evaluated earlier[3] was successfully employed in both of these models, it was foreseen that additional investigations would be necessary to determine the sensitivity of nozzle shape, nozzle size, and cam eccentricity on the performance of the pneumatic valving system and the effect of these parameters on pressure loss characteristics. To obtain this information, the rotor mast employed for the previously mentioned rotor investigations was used as a test apparatus. Additionally, information was obtained on the total pressure losses of a contraction section located between the nozzle and the blade entrance and, to a limited extent, the effect of downstream slot area.

---

[1] Wilkerson, J.B. et al., "The Application of Circulation Control Aerodynamics to A Helicopter Rotor Model," Paper 704, 29th Annual Forum of American Helicopter Society, Washington, D.C. (10-11 May 1973).

[2] Wilkerson, J.B. and D.W. Linck, "A Model Rotor Validation for the CCR Technology Demonstrator," Paper 902, 31st National Annual Forum of the American Helicopter Society, Washington, D.C. (May 1975).

[3] Reader, K.R., "Evaluation of A Pneumatic Valving System for Application of A Circulation Control Rotor," NSRDC Report 4070 (May 1973).

MODEL AND EQUIPMENT

MODEL DESIGN

The rotor head and one of the blades of the higher harmonic circulation control (HHCC) rotor model were used to evaluate the pressure losses across various combinations of seven nozzles and five cams. A cam-adjusting mechanism was designed to enable rapid adjustment of the cams azimuthal position. The adjusting mechanism, which was mounted on top of the rotor head, allowed for the quick installation or removal of either the cams or nozzles. Photographs of experimental arrangement and model details are presented in Figure 3. The nozzles, which were mounted in the rotor head, ran on a 3.5-in.-diameter circle with a cam mounted in the center. The gap between the cam and nozzle provided the varying control area which modulated the pressure and mass flow. In principle, the operation is the same as that reported earlier.[3] Blade 1 from the HHCC rotor model was used as a downstream receiver and provided a downstream slot area of 0.413 in^2.

The design of the nozzles was such that the effect of nozzle shape and size could be evaluated. The basic shapes of the nozzles were rectangular and circular. The four rectangular nozzles tested were selected from a list of 12 different planforms and represent the minimum number that could be used to determine a change in performance due to aspect ratio and size. The aspect ratios of the rectangular nozzles ranged from 0.5 to 2.0, and their total area ranged from 0.32 to 2.25 in^2. The three round nozzles selected were the largest that could conventiently fit into the rotor hub, the smallest that was compatible with the blade inlet area, and one in between these extremes. The circular nozzles had diameters of 1.0, 1.33, and 1.75 in. with respective areas of 0.78, 1.39, and 2.40 in^2. Only one of the rectangular nozzles had a contraction piece immediately downstream of the nozzle, but all three of the circular nozzles had contraction pieces. The contraction pieces are transition sections which help to streamline the airflow between the nozzles and the downstream receiver. Detailed dimensions and shapes of the nozzles and contraction pieces are presented in Figure 4, and photographs of the nozzles are included in Figure 5.

A pair of endplates was designed so that Nozzle 1 could be used to evaluate the effects of three-dimensional mixing in the rectangular nozzles. The endplates overlapped the cam and sealed against it so that flow was controlled only by the side of the nozzle (see Figure 3)

The HHCC cam (Cam 5) plus four others were used to evaluate the effect of cam eccentricity on the pressure losses across the cam-nozzle valve. The five cams were systematically designed to cover a range of maximum cam throw from 0.056 to 0.314 in. The cams were tested by using Nozzle 1 with a contraction piece between the nozzle and blade inlet. Details of the various cams are presented in Figure 6, and photographs are shown in Figure 7.

MODEL CONSTRUCTION

The rotor mast (this includes all of the model except the blades) and Blade 1 of the HHCC rotor model served as test apparatus to evaluate the various nozzles and cams. A cam-adjusting mechanism was manufactured to enable the azimuthal positioning and axial positioning of the cam with respect to the centerlines of the nozzles. A dummy steel control shaft was used to hold the cams in proximity to the nozzle within the head. This shaft passed through a plexiglass top and had a drum indicator attached to enable accurate measurement of the cams azimuthal position with respect to the nozzle centerline. The cam which was screwed to the shaft and the dial indicator which was attached by set screws had relative adjustments which enabled these components to be aligned with the centerline of the nozzle. Also passing through the top was a total pressure probe. A photograph of the cam-adjusting mechanism is shown in Figure 3c.

The nozzles were designed to be compatible with the rotor head. Nozzle 1, which was rectangular in shape, was the same nozzle used in the HHCC rotor model and was fabricated from steel with an aluminum contractor. The other rectangular shaped nozzles (2-4) were fabricated from wood and did not have contractors. The circular nozzles (5-7) were fabricated from plexiglass, and each had its own plexiglass contractor. The inlet of all seven nozzles had a 3.5-in. diameter radius which

coincided with the center of rotation of the rotor mast. The nozzle inlet had a sharp inside edge, and the outside edge had a 3/15-in. radius. The top and bottom edges of the rectangular nozzles, however, were curvilinear and had sharp inside and outside edges; see Figures 4 and 5.

One of the cams (Cam 5) had previously been used in the HHCC rotor model, and a typical pressure loss curve was already available.[2] This cam was constructed from aluminum. The other four cams were fabricated from plexiglass and designed so that the maximum radius coincided with the 3.5-in. diameter of the nozzles. There was a nominal minimum gap of 0.010 in. between the nozzle and the cam. This value varied slightly depending on which cam and/or nozzle was installed. The shape of Cam 5 was cut to give a sinusoidal area variation; this cam had a radius whose governing equation was

$$R = R_o + R_1 (1 + \text{Sin } \psi)$$

where R_o = minimum radius

R_1 = mean eccentricity of the cam

ψ = azimuthal angle

Cams 1-4 were cylinders with offset centers to make them eccentric. This method of manufacture did not greatly compromise the sinusoidal area variation. It can be shown that the radius for the offset center on a circle approximates the pure sinusoidal radius variation within 5 percent for the cam with the largest throw. The variation of radius of the other cams was less than this; see Figures 6 and 7 for details and photographs.

INSTRUMENTATION

The hub total pressure was measured by using a T-shaped probe which was connected to a differential pressure gage (Wallace and Tiernan) calibrated in inches of mercury and a $\pm$15-psid Statham pressure transducer. The blade inlet total pressure was measured by a 25-psia Kulite pressure transducer. A wall static pressure tap was installed at the blade inlet and a pitot-static tube was mounted approximately 5 in. from the tip of the blade. These three pressures were measured by means

of ±15 psid-Statham pressure transducers. The mass flow was measured for each data point by using a venturi meter. The signals from the pressure transducers and the information necessary to calculate mass flow were recorded on magnetic tape by means of a Beckman 210 analog to digital converter. From these magnetic tapes, the data were reduced to coefficient form by an XDS 930 computer. The output from the computer was automatically plotted by a Calcomp plotter.

PROCEDURE

In the period from October to February 1972, seven nozzles and five cams were evaluated to determine the effect of nozzle shape, nozzle size, and cam eccentricity on the pressure losses across a cam-nozzle valve system. The hierarchy of test parameter is (1) configuration (i.e., a particular nozzle and cam), (2) hub pressure, and (3) cam azimuth position. The test consisted of systematically changing the model configuration and then varying the hub pressure and cam azimuth position. The discrete azimuth position method[3] was the technique used to obtain the data presented in this report. The range of hub pressure tested was 2 to 15 psig, and the cam azimuth position was varied in 30-deg increments from 0 to 360 deg. A test program of configurations evaluated is presented in Table 1.

RESULTS AND DISCUSSION

CAM ECCENTRICITY

The effect of various cam eccentricities on the total pressure loss was determined by using the five previously described cams. Data were obtained for a range of cam-eccentricity to cam radius (e/r) of 0.0164 to 0.0998. Nozzle 1 and its contractor were used in conjunction with the HHCC rotor blade (Blade 1) for all five cams. Everything in the physical system was held constant except for the five cams. Figure 8 shows the total pressure loss coefficient versus the nondimensional area coefficient A_c/A_s. Note the very good agreement for all five cams. The implication is that within the constraints of this investigation,

varying the eccentricity of the cam had no effect on the characteristic curve of total pressure loss versus area coefficient.

NOZZLE SIZE AND SHAPE

Another important component of the valve, the nozzle, was varied in size and cross-sectional shape to evaluate the effect of such changes on the pressure loss-area characteristic curve. As stated earlier, both rectangular and circular nozzles were evaluated, some with and some without contraction pieces. For particulars on the nozzle, see the section on model design and Figure 4.

Figure 9 indicates the effect of the various nozzle configurations on the pressure losses between the hub and blade. Figure 9a includes all of the nozzle configurations which were evaluated with contraction pieces, and Figure 9b includes all nozzle configurations evaluated without contraction pieces. The faired curve in Figure 9a and the dashed curve in Figure 9b are the same faired curve presented in Figure 8. The good agreement between the various nozzle data indicates that no trouble should be encountered in changing the cross-sectional shape or the size of a nozzle.

In nozzle design, it is generally necessary to adequately fair the region between a large cross-sectional area and a smaller one (and vice versa), but sometimes the proper design criteria (i.e., contractor shape, diffuser angle, and length) cannot be upheld. It is then more feasible, both economically and for pressure recovery gains, to have an abrupt contraction or diffusion. The removal of the contraction piece causes a relatively large diffusing or contracting section just before the blade entrance. The seven nozzles were accordingly evaluated with abrupt cross-sectional area changes between the nozzle and the blade entrance. The overall pressure and mass flow rate in the far downstream section remained established, but the abrupt diffusion and contraction caused local flow problemswith pressure-measuring devices in the smaller inlet region. For example, when Nozzle 2 was tested without a contraction piece (this nozzle had the smallest area), the pressure measurement was incorrectly indicated because the flow at the blade entrance was completely erratic.

This condition was observed for hub pressures greater than 2 psig and not observed for any other configuration tested.

Figures 9a and 9b respectively depict streamlined and unstreamlined flows; the matching symboled data in the two figures can be used to evaluate the effect of streamlining in the region between the nozzle and the blade inlet. Based on these data, cross-sectional streamlining is not considered to affect pressure recovery until the area coefficient is 1.4 or greater, and even then the reduction in pressure recovery is only marginal.

It is reasonable to assume that a three-dimensional flow is present in the rectangular nozzles because the flow enters from all four sides of the nozzle. To determine the extent to which the bottom and top flows of air into the nozzle were generating mixing losses, a set of endplates was mounted on the bottom and top of Nozzle 1. A comparison of the nozzle with and without endplates indicated a substantial amount of mixing is being done in the nozzle. This mixing was manifested in the form of a relatively large pressure loss between the hub and the blade; see Figure 10.

DOWNSTREAM SLOT AREA

A sideline of this investigation called for obtaining some preliminary data that would enable an evaluation of the effect of downstream slot area. This was rather important in that the downstream area is the nondimensionalizing factor in the area coefficient. Two round holes were hand drilled normal to the upper surface and 9.0 in. from the tip of the HHCC rotor blade. The diameters of the smaller and larger holes were respectively 0.316 and 0.500 in., which amounted to an increase in geometric area of 19.0 and 47.5 percent, respectively. When the total pressure loss coefficients were compared as a function of area coefficient, the shape of the curve seemed correct but the curves were shifted to the right. The round holes that were drilled for the additional exit area were estimated to have a discharge coefficient between 0.5 and 0.7 depending on hole geometry. A discharge coefficient of 0.85 was applied to the total exit area (slot area plus hole area) in order to correlate

the data. This amounted to a discharge coefficient of 0.53 for the additional holes (see the appendix). The correlated data are presented in Figure 11 along with the reference curve established in Figure 8. The value of 0.85 was applied to both sets of data, and no attempt was made to establish the best correlation for each separate set. The important thing is that the data correlated well with the simple parameter $1/\eta_o$ where $\eta_o = 0.85$.

AREA COEFFICIENT

Data from several models were used as a check on the area coefficient as a correlating parameter between various configurations. These data are from an experiment reported earlier[3] and from several CC rotor models tested at DTNSRDC over the past several years. Figure 12 shows that as the downstream exit area decreases, the curves maintain the same basic shape but shift to the left. The same physical arrangement was used to hold the cam relative to the nozzle for the CCR1,* CCR2,* and HHCC models. The looseness of the cam rod installation enabled the cam to move approximately 0.006 in. to and from the nozzle. When resolved into an area coefficient, this displacement amounts to a 14-percent change in A_c/A_s for the CCR models and about a 6.5-percent change for the HHCC model. An examination of Figure 12 shows that the spread of the curves was within this tolerance. The only difference between the CCR1 and CCR2 models was a slight change in the downstream exit area; in contrast, exit area and cam eccentricity were twice as large for the HHCC model as for the CCR models. The data from the original pipe model did not correlate well. However, these data represent the largest change in slot configuration presented in Figure 12. The cam and nozzles used in the original pipe model and the HHCC model had the same eccentricity, but, the downstream exit area and exit area contours varied drastically.

An examination of the downstream exit area contours explains why complete correlation could not be achieved. Figure 13 shows slot contours

*CCR1 and CCR2 are designations of different internal slot geometries for blades used on the CCR model. The geometry of the two slots is shown in Figure 13.

for all of the models for which data are included in Figure 12. The CCR models and the HHCC model all had well-contoured trailing edge slots with a discharge coefficient very close to 1.0. The original pipe model had a brass tube (wall thickness of 0.125 in.) with a machined parallel wall slot, which was adjusted to a slot height of 0.042 in. The slot configuration had parallel sides for a relatively long distance compared to the slot height. The establishment of a vena contracta in the parallel section effectively reduced the slot area, thereby shifting the curve to the right. Included in Figure 12 as a dashed curve are data established as a reference in Figure 8, for which the variation of the control area was much smaller. Although the data in Figure 12 do not enable the data correlation to be completed, they do point up three important things:

1. All of the data were within the range of accuracy of the dashed reference curve when control area variations were considered.

2. The shape and slopes of the curves were the same for all of the curves.

3. No major problem would be encountered when using the reference curve for the design of other cam valve systems.

PRESSURE LOSS COEFFICIENT

The mechanical principle used to modulate the total pressure in the rotor blade is to introduce variable losses between the hub plenum and the blade in a controlled and predictable fashion. In Reference 3 a loss coefficient K_A was defined by the equation:

$$K_A = \frac{\Delta P_T}{q}$$

where ΔP_T is the hub plenum total pressure minus the blade inlet total pressure, and the dynamic pressure is at the blade entrance, therefore

$$K_A = \frac{P_h - P_b}{P_b - p_b}$$

The most convenient form of pressure data from the rotor system are the hub total plenum pressure and blade entrance total pressure. Therefore a more easily definable pressure loss coefficient was defined as

$$K_R = \frac{P_B - p_\infty}{P_H - p_\infty} = \left.\frac{P_b}{P_h}\right)_{gage}$$

where $(P_H - p_\infty)$ is a dynamic pressure based on expanding the hub total pressure to atmospheric pressure and $(P_B - p_\infty)$ is the difference between the blade entrance total pressure and the atmospheric pressure. As shown above, this loss coefficient is the ratio of hub plenum gauge pressure and blade entrance gauge pressures, both values that are directly obtainable from the rotor instrumentation.

It can be shown that if K is the loss coefficient based on the dynamic pressure of the nozzle and K_1 is the loss coefficient based on the dynamic pressure of the exit slot, then:

$$K = K_1 \left(\frac{A_c}{A_e}\right)^2$$

The relationship between K_R and K can be shown to be:

$$K_R = \frac{1}{1+K\left(\frac{A_c}{A_e}\right)^2}$$

K_R is the pressure loss coefficient used throughout this report.

Figure 14 presents plots of loss coefficient versus cam azimuthal position. Figure 14a is for all five cams in proximity to Nozzle 1 (W/H = 0.5) and shows that as the eccentricity increased, the maximum pressure ratio decreased. Figure 14b and 14c are respectively for the nozzle configurations with and without contractors. Streamlining the transition region between the nozzle and blade entrance caused only a small change in the shape of the loss coefficient curve (compare the curves for the same nozzles in Figures 14b and 14c). The cross-plotting

of the maximum loss coefficient from Figure 14a yielded a maximum limit of the loss coefficient as a function of cam eccentricity. This curve (Figure 15) shows that there was a definite eccentricity range and that beyond it, the top of the loss coefficient versus azimuth position curve flattened.

HARMONIC ANALYSIS

The cam-nozzle relationships are designed to provide specific harmonic input to the blades for rotor control and vibration suppression. The curves of loss coefficient versus azimuth position provide a subjective evaluation of the blade pressure wave but not a qualitative evaluation of its content. The harmonic analysis of the blades' pressure, mass flow rate and jet velocity gives this qualitative evaluation of what the actual harmonic content of these parameters are in the blades. The curves in Figure 14a were harmonicly analyzed and then normalized by the 1P component. The 1P component was chosen for normalization because it was the most important and predominate harmonic.

Figure 16 shows the harmonic content of the loss coefficient and the mass flow for the various cam configurations. Note the strong 2P component in the loss coefficient beyond the limiting eccentricity indicated in Figure 15. For the pressure loss coefficient, the analysis shows that above the 2P frequency, the magnitude is small enough to be neglected. The harmonic content of the mass flow data shows that the higher harmonic was much more prevalent in the mass flow. Figure 16b shows that the 2P and the 3P were fairly large compared to the basic 1P for which the cam was cut. This suggests that in order to control the higher harmonic input, a more restrictive limitation needs to be placed on the limiting value of the ratio of control area to slot area. A cross-plot of the loss coefficient (Figure 17) and mass flow (Figure 18) data versus cam eccentricity shows that an eccentricity of 0.056 in. is best to reduce the 2P content in the pressure term whereas the smaller the eccentricity the better, so far as mass flow is concerned. For the pressure, the 3P component is about constant with cam eccentricity while

the mass flow minimizes at an eccentricity of about 0.056 in. Included are data for the configuration where holes were drilled to obtain additional downstream slot area. These data substantiate the pure slot exit data.

The normalized harmonic content of loss coefficient, mass flow rate, and jet velocity for a nozzle aspect ratio of 0.5 (Nozzle 1) is presented in Figure 19. The loss coefficient and mass flow rate data are for the same configuration as presented in Figure 16 for Cam 5. The jet velocity was calculated by using the isotropic expansion of the air through the slot. The equation for this calculation is:

$$V = \{2RT_d \quad (\gamma/\gamma-1) \; [1-(P_\infty/P_d)^{\gamma-1/\gamma}]\}^{1/2} \qquad (1)$$

The jet velocity was harmonically analyzed and the components normalized by the 1P term. The results are plotted in Figure 19c. As expected, the higher harmonic jet velocity components were about the same as for the mass flow rate. Hub pressure had a minimal effect on the harmonic content of loss coefficient, mass flow, and jet velocity; see Figures 19 and 20. The data presented in Figures 21a and 21b were normalized by the constant term instead of the 1P term. The data of Figure 21 show that although the pressure exhibited mostly 1P, the mass flow rate showed a substantial amount of collective mass flow with a reduced amount of 1P component. The harmonic analysis of the mass flow rate and loss coefficient curves showed no effect on the harmonic content for the configurations without a contractor between the nozzle and blade entrance.

CONCLUSIONS

Several conclusions have been drawn:

1. Cam eccentricity had no effect on the total pressure loss versus area characteristic curves.

2. The good agreement between the various nozzle data indicated that no stringent requirements should be encountered in changing the cross-sectional shape or the size of the nozzle.

3. Streamlining the transition section between the nozzle and blade entrance did not affect pressure losses until the area coefficient was 1.4, and then the reduction in pressure losses was only marginal.

4. Streamlining the transitional region between the nozzle and the blade entrance had minimal effect on the shape of the loss coefficient curve and no effect on the harmonic content of the loss coefficient or mass flow rate.

5. The addition of endplates to the nozzle reduced the amount of mixing in the nozzle, thereby reducing the total pressure losses between the hub and the blade.

6. Two parameters were shown to be adequate to correlate data for different models, namely, the area coefficient (the control area divided by the downstream exit area) and the total pressure loss coefficient (the blade total entrance gage pressure divided by the hub total gage pressure).

7. For a consistent set of data, the harmonic analysis of the pressure loss coefficient agreed with the cam input but the harmonic analysis of the mass flow rate contained a significant amount of higher harmonic. The harmonic analysis of the jet velocity was approximately the same as the mass flow rate.

8. Hub pressure had a minimal effect on the harmonic content of the pressure loss coefficient, mass flow rate, and jet velocity.

APPENDIX

CALCULATION OF DISCHARGE COEFFICIENT

This section presents the method used to correlate the data for the slot plus the additional round holes with the data for the slot only. The data were correlated by using a general lumped parameter which was equal to $\eta_o = 0.85$.

In the equations which follow,

A_s = the geometric area of the slot

A_h = the geometric area of the drilled holes

A_t = the geometric area of the total exit

A_c = the correct area accounting for discharge coefficient

A_e = the true effective exit area

η = discharge coefficient

$$A_t = A_s^* + A_h \tag{1}$$

$$A_c = A_s^* + \eta A_h \tag{2}$$

The asterisk indicates for well designed slots $\eta = 1.0$.

To correlate, the following equation was used

$$A_e = 0.85\ A_t \tag{3}$$

To solve for η, equate (2) and (3) and solve for η

$$\eta = \frac{0.85\ (A_s + A_h) - A_s}{A_h} \tag{4}$$

Evaluating η for the smaller hole (D = 0.316 in.) by using Equation (4), $A_s = 0.413$ and $A_h = 0.0784$ gives

$$\eta = 0.533$$

Evaluating η for the larger hole (D = 0.500 in.) by using Equation (4), $A_s = 0.413$ and $A_h = 0.1964$ gives

$$\eta = 0.534$$

These numbers are what would be expected for holes which were drilled through fiberglass and 1/16-in. steel plate with no attempt at cleaning or shaping the holes.

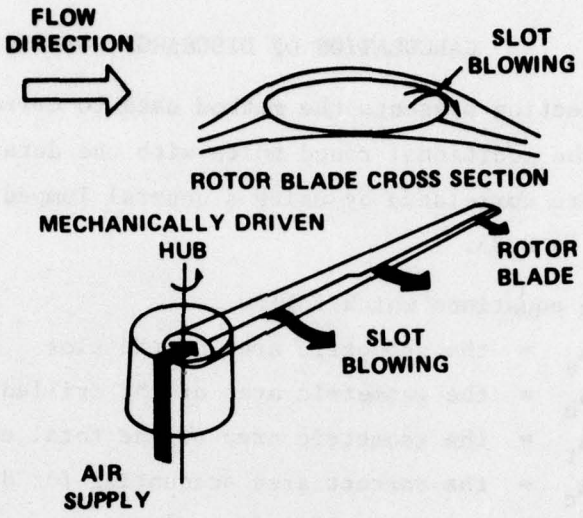

Figure 1 - Basic Circulation Control Concept

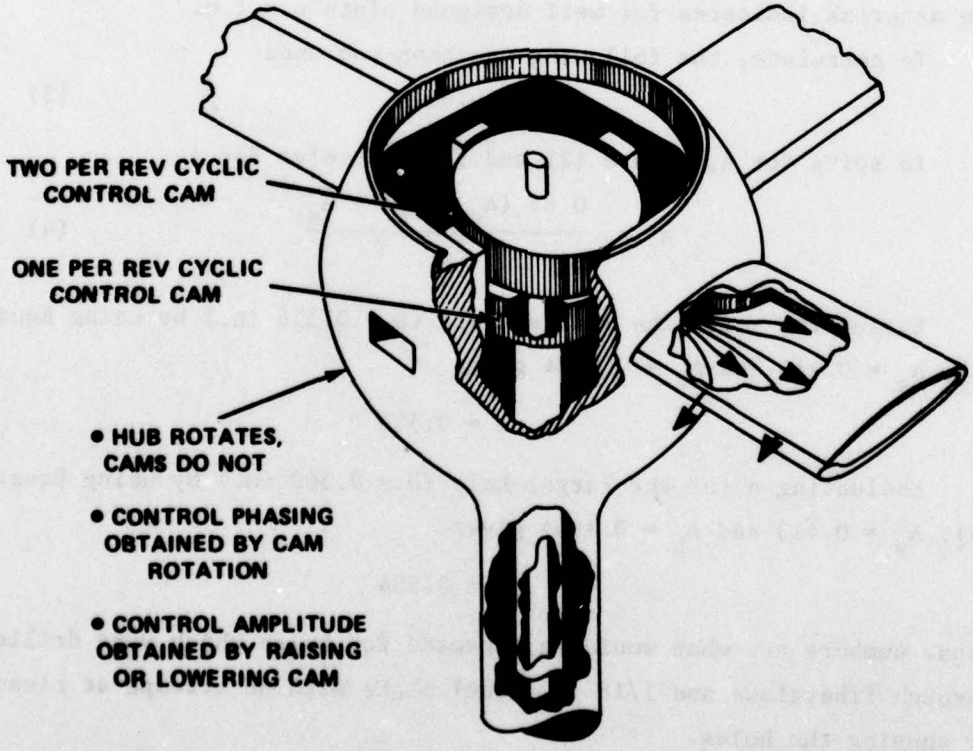

Figure 2 - Circulation Control Rotor Hub

Figure 3 - Model Details and Experimental Arrangement

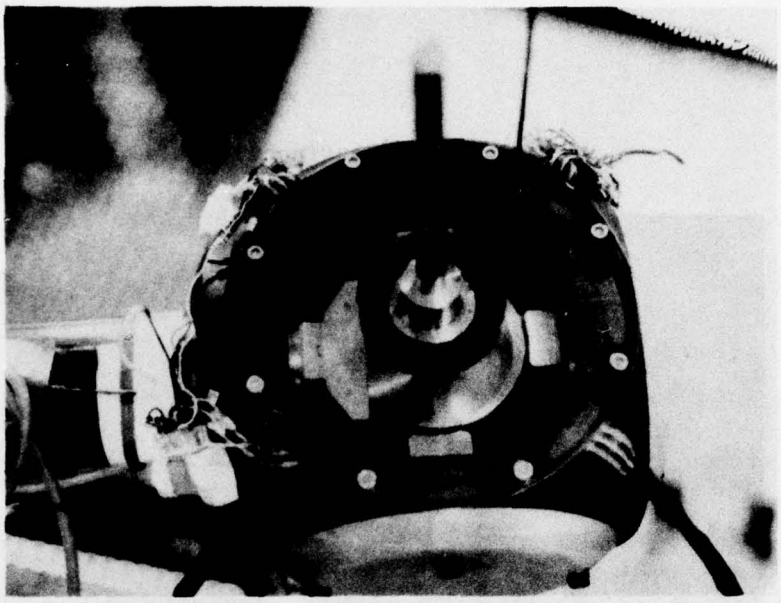

Figure 3a - Model Details

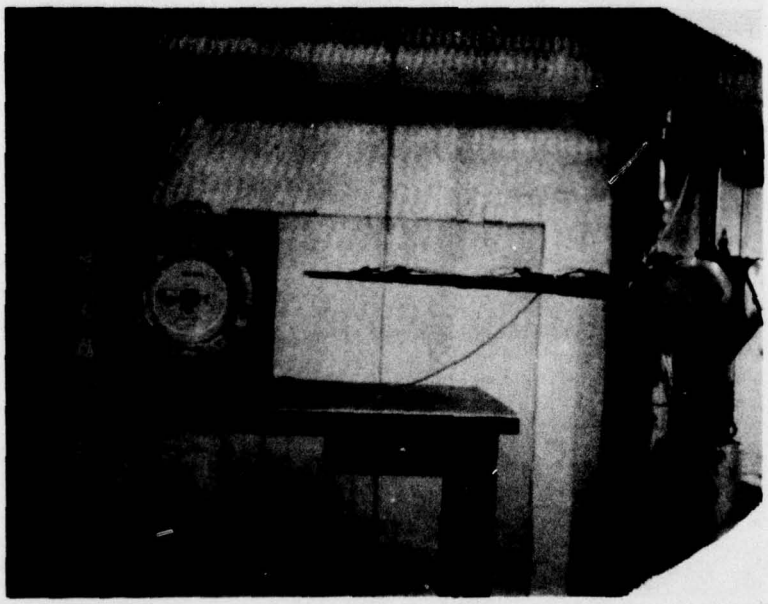

Figure 3b - Experimental Arrangement

Figure 3 (Continued)

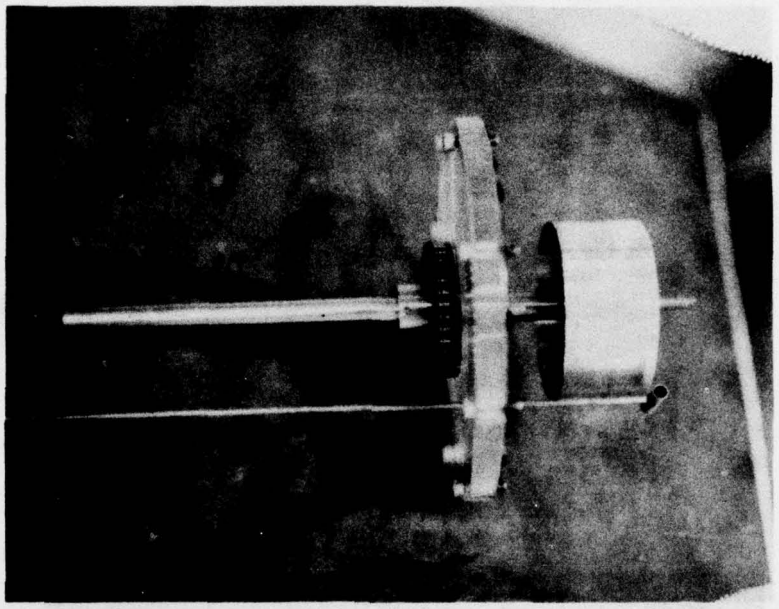

Figure 3c - Cam-Adjusting Mechanism

Figure 4 - Details of Nozzles and Contraction Pieces

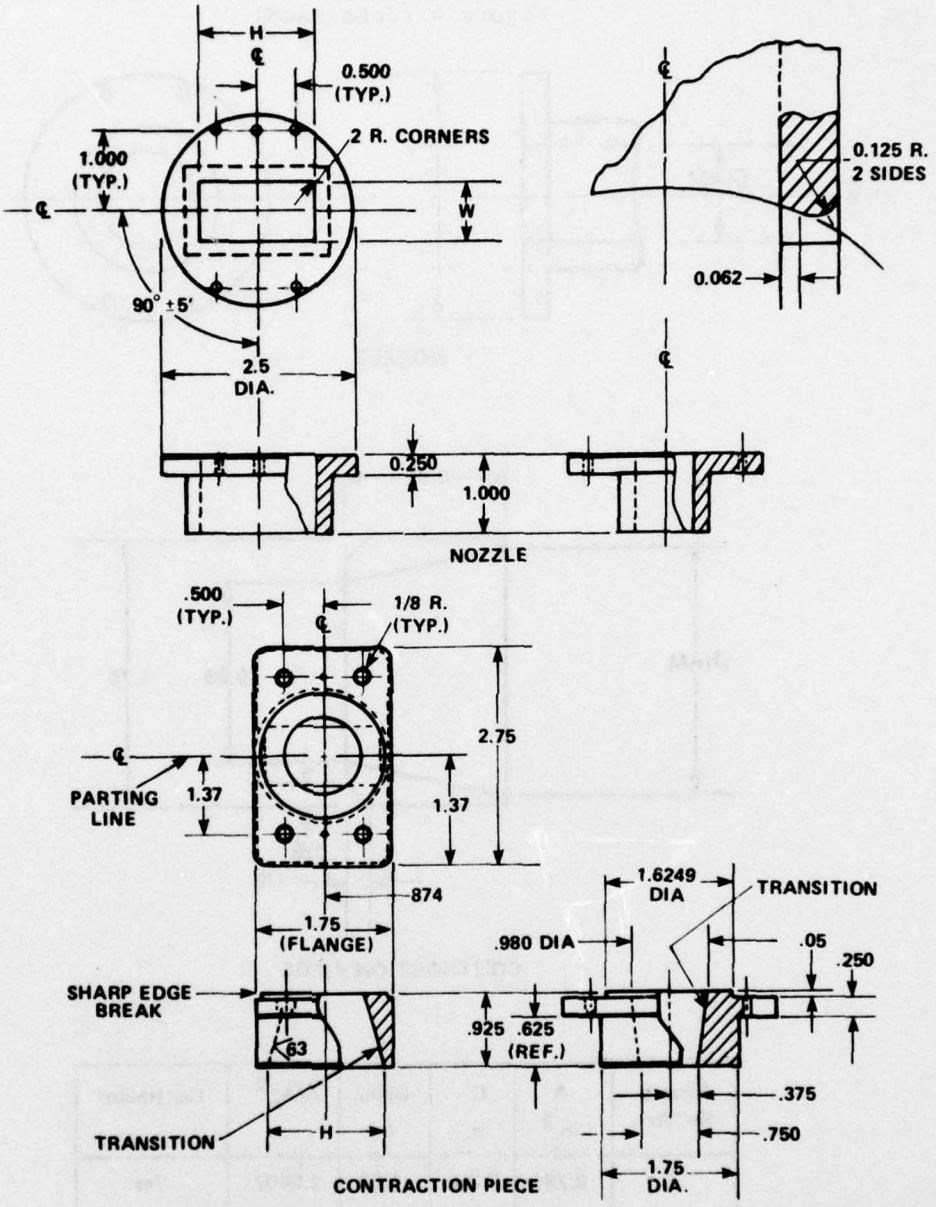

Nozzle Number	A in.^{2}	C[1] in.	W in.	H in.	W/H	Contractor
1	1.125	4.50	0.75	1.5	0.5	Yes
2	0.3164	2.25	0.5625	0.5625	1.0	No
3	1.125	4.50	1.5	0.75	2.0	No
4	2.25	6.0	1.5	1.5	1.0	No

[1] C = 2 (W + H).

Figure 4a - Rectangular Configurations

Figure 4 (Continued)

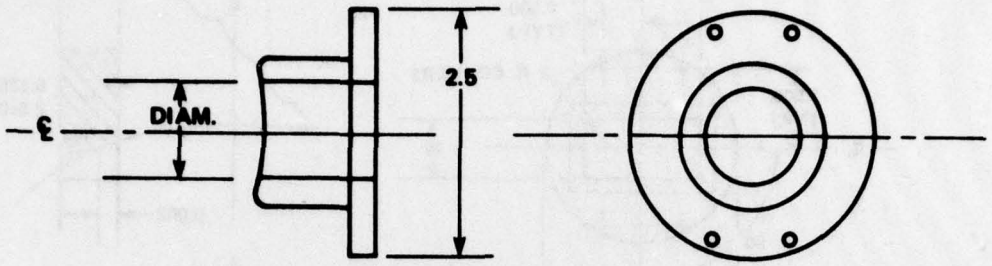

NOZZLE

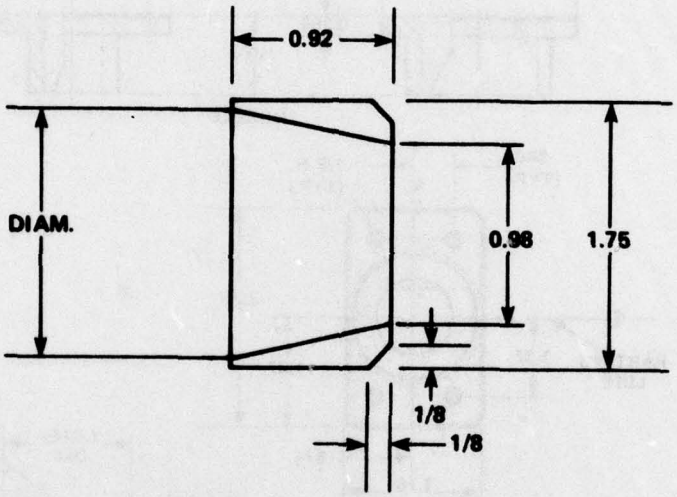

CONTRACTION PIECE

Nozzle Number	A $in.^2$	C in.	Diam. in.	A/A_o^2	Contractor
5	0.785	3.29	1.00	1.0407	Yes
6	1.389	4.32	1.33	1.8414	Yes
7	2.405	5.65	1.75	3.1884	Yes

[1] $C = \pi$ Diam. + 0.1433.

[2] $A_o = 0.7543$ in.

Figure 4b - Circular Configurations

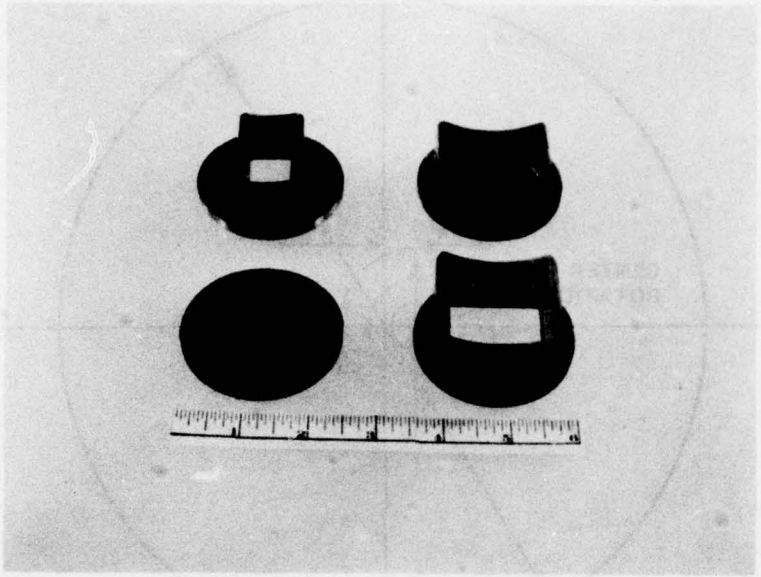

Figure 5a - Rectangular Nozzles

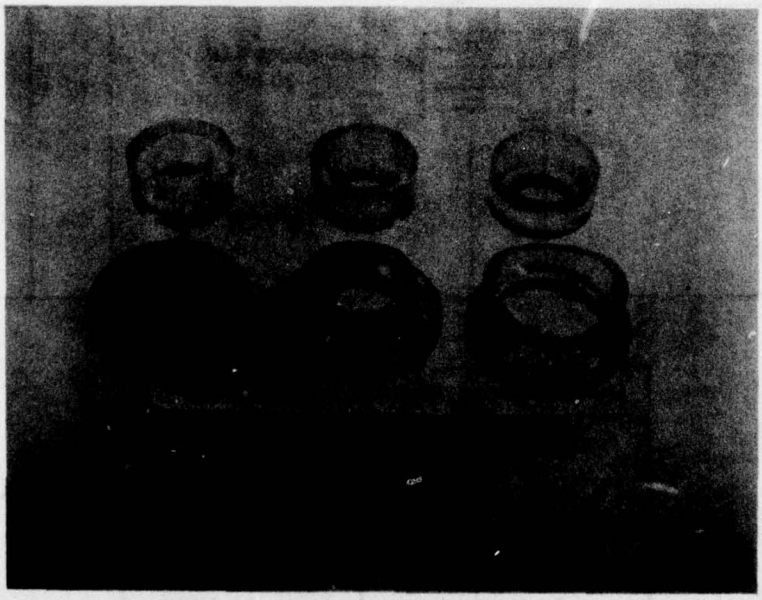

Figure 5b - Circular Nozzles

Figure 5 - Types of Nozzles

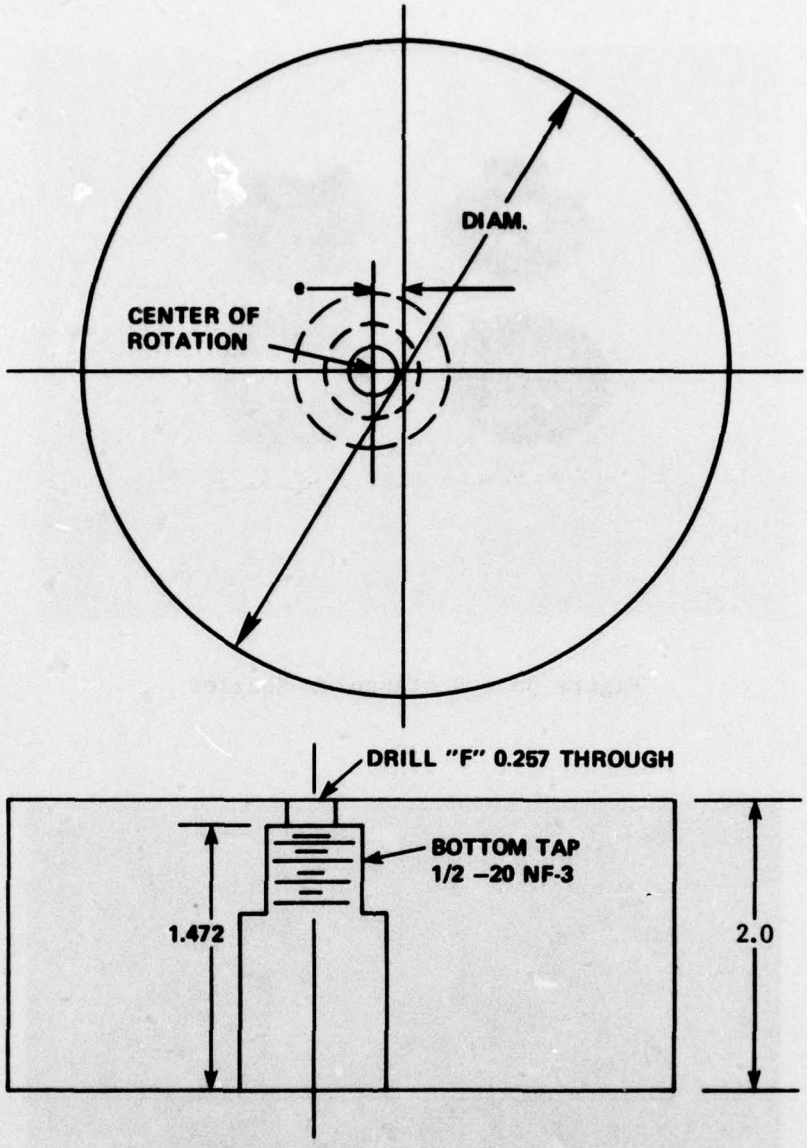

Cam Number	Diam.	e	e/r
1	3.146	0.157	0.0998
2	3.368	0.056	0.0333
3	3.396	0.042	0.0247
4	3.420	0.028	0.0164
5	3.248	0.111	0.0683

Figure 6 - Detail of Various Cams
(All dimensions are in inches)

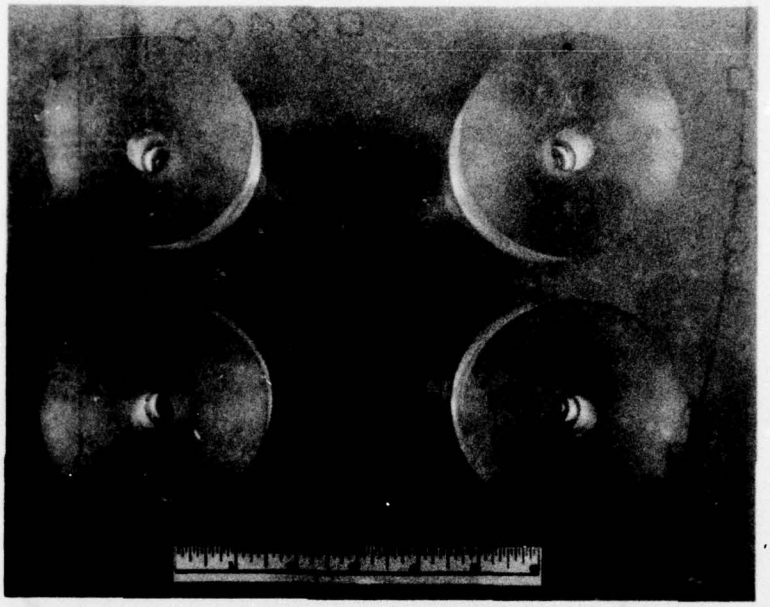

Figure 7 - Types of Cams

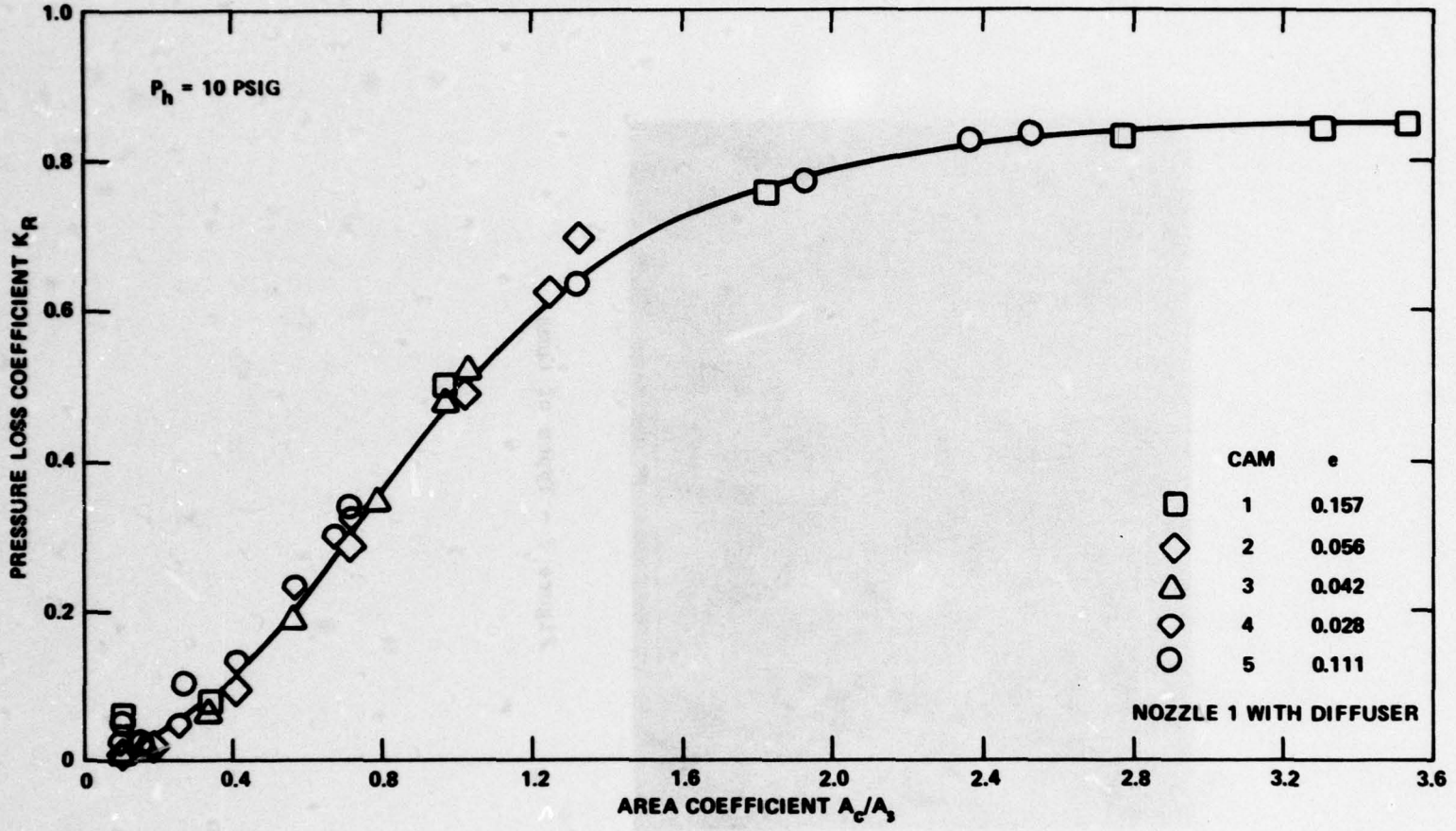

Figure 8 - Effect of Cam Eccentricity

(See Figure 6 for cam details)

Figure 9 - Nozzle Effect

(Nozzle details are given in Figure 4
and cam details in Figure 6)

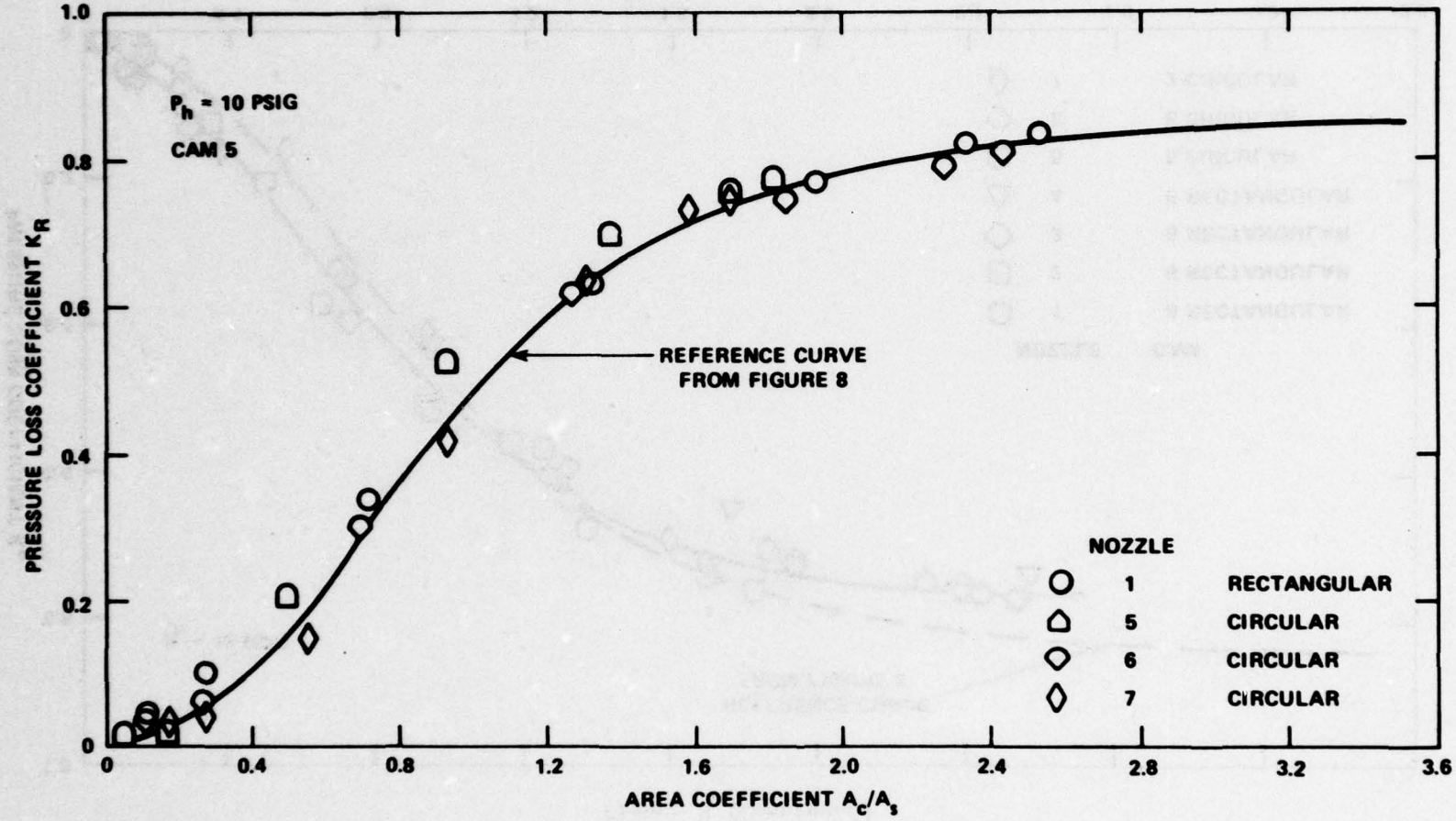

Figure 9a - With Contraction Piece

Figure 9 (Continued)

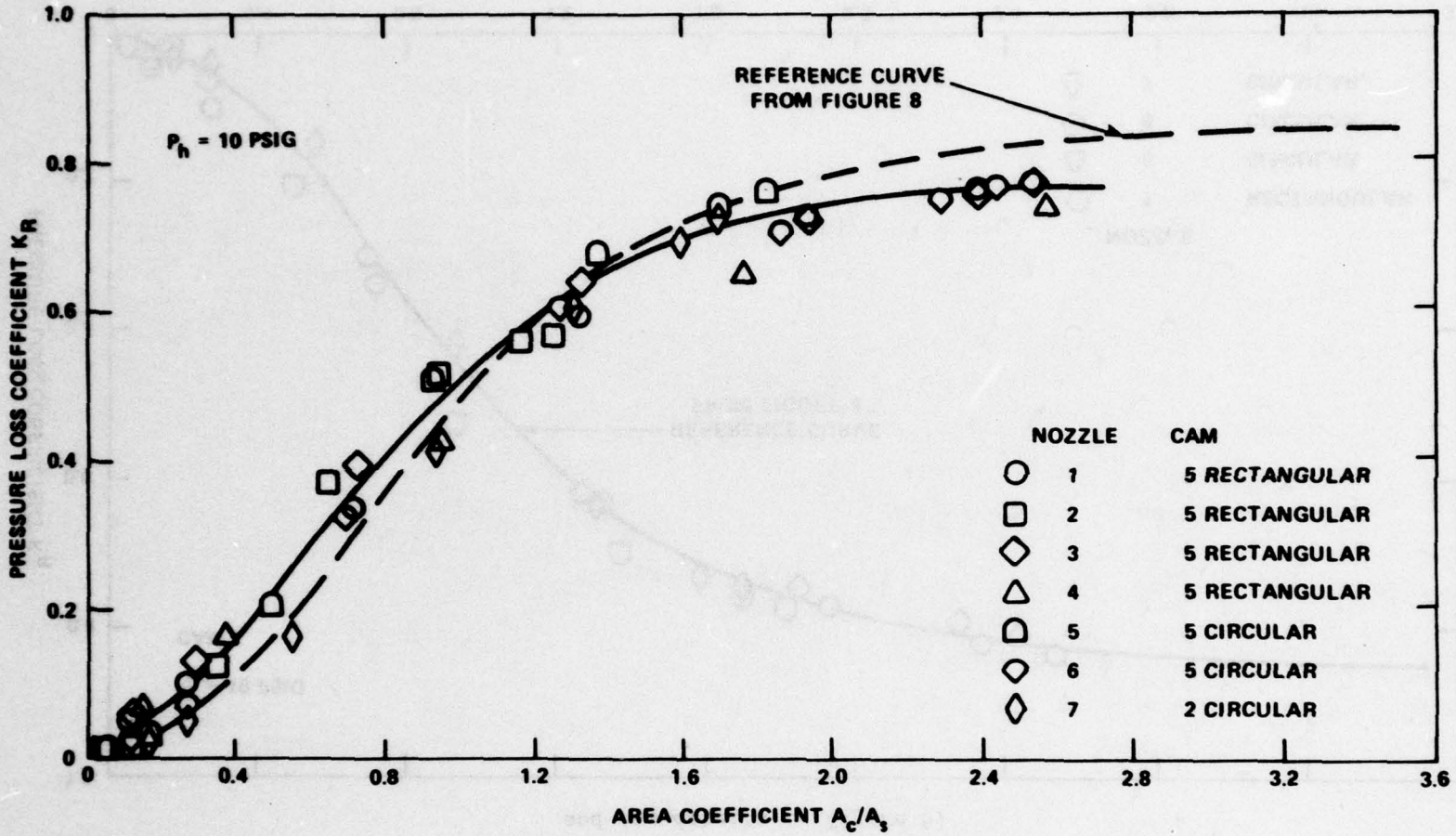

Figure 9b - Without Contraction Piece

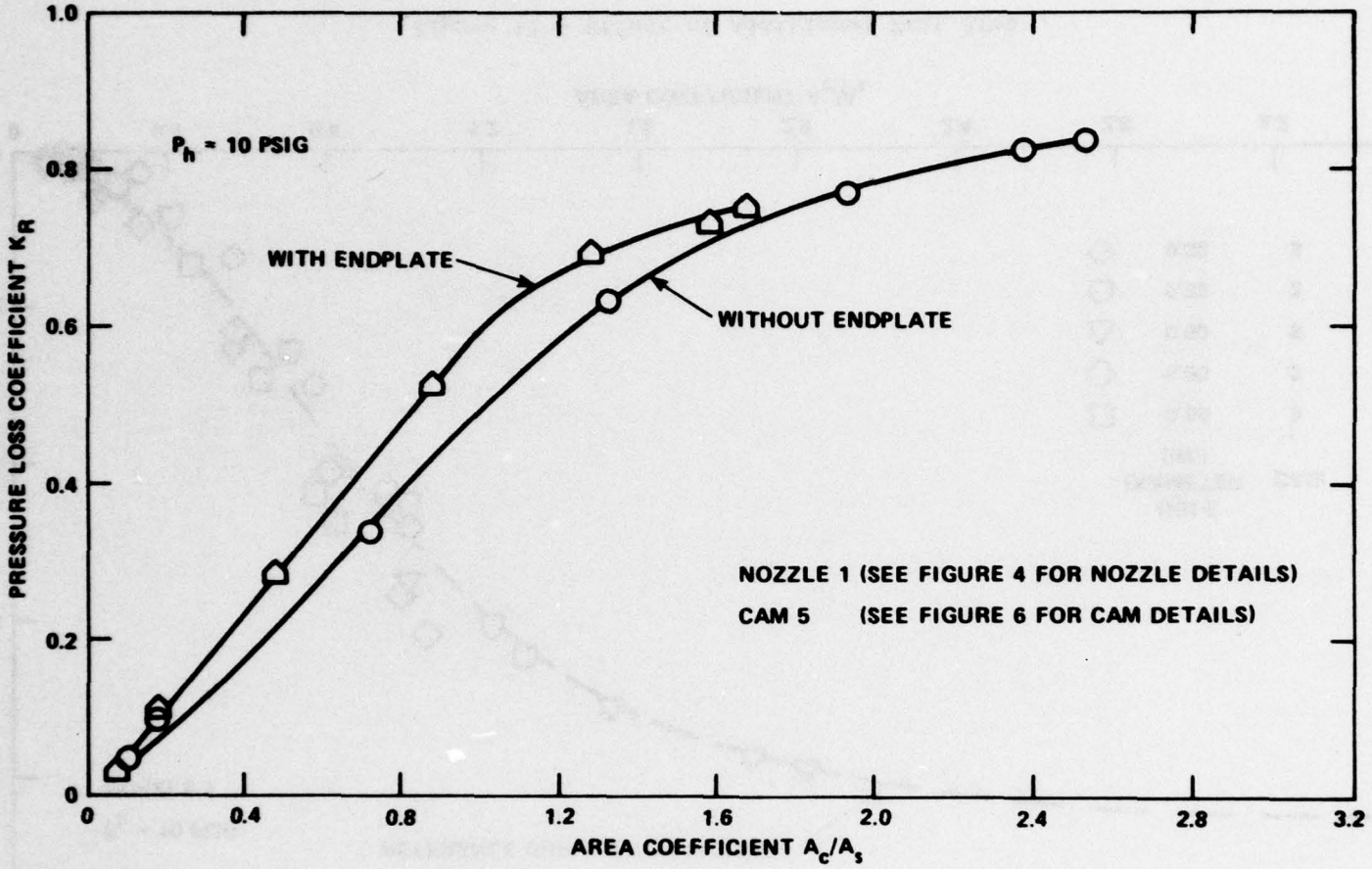

Figure 10 - Effect of Endplates on Nozzle

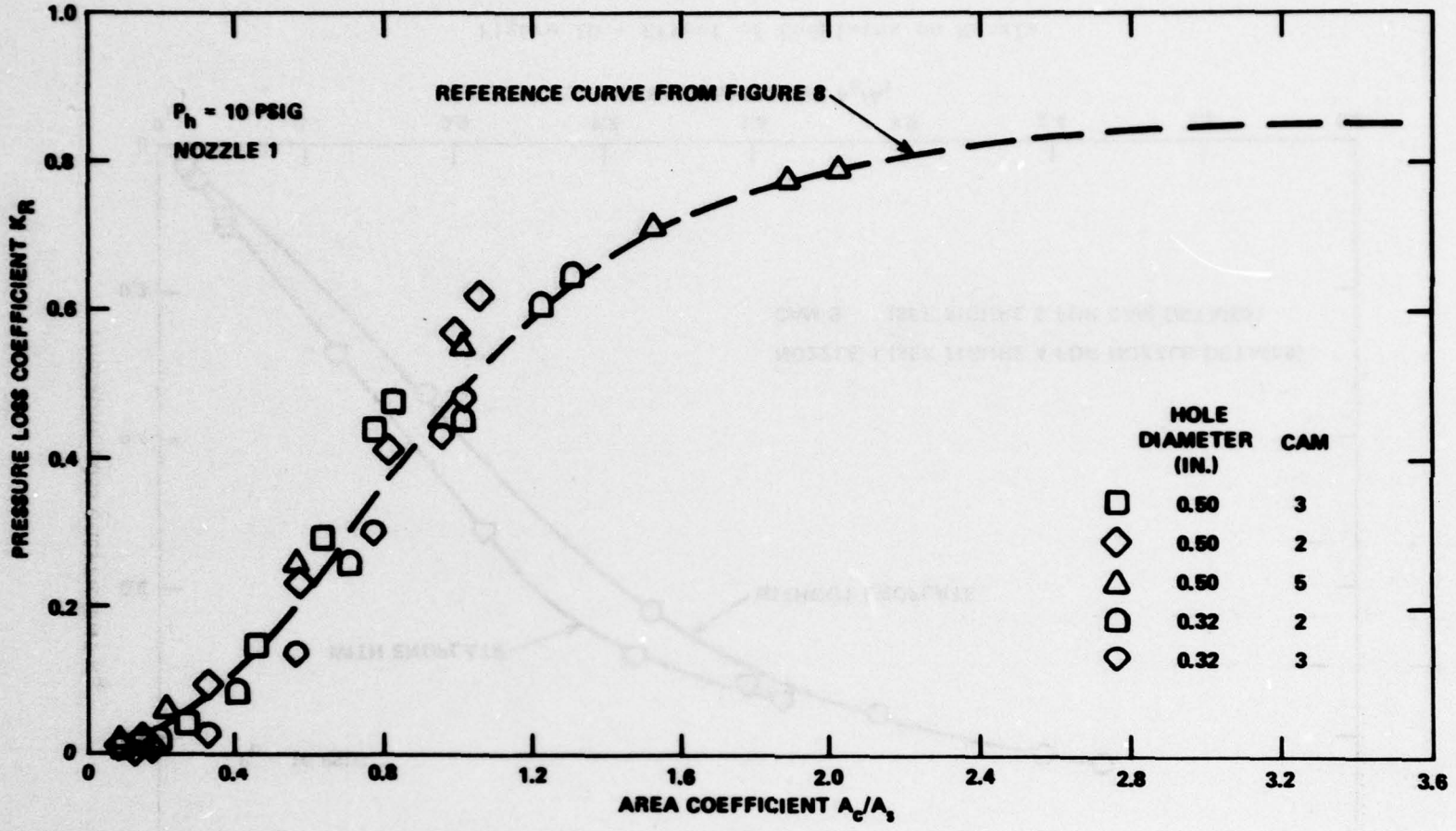

Figure 11 - Effect of Additional Exit Area

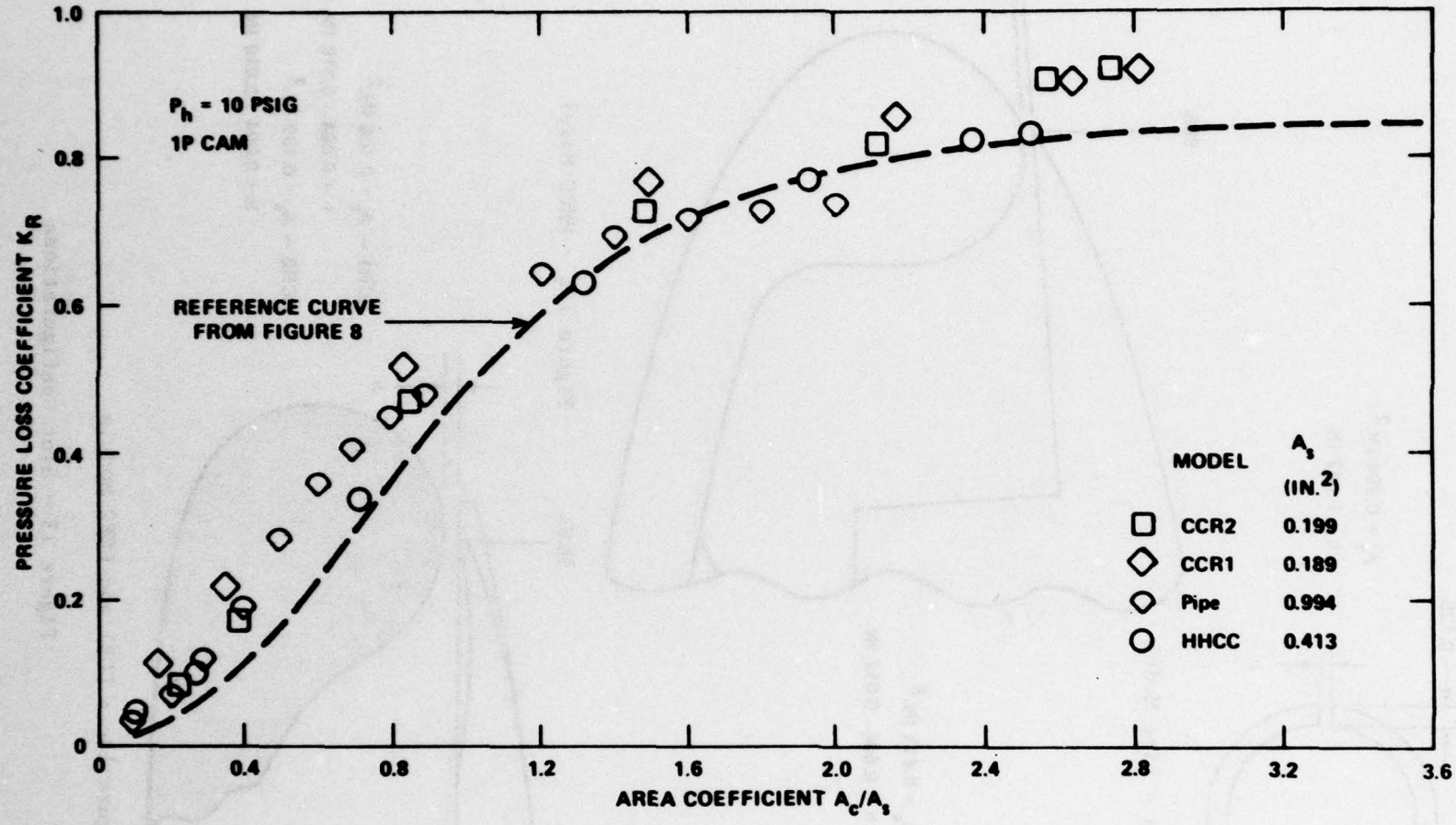

Figure 12 - Effect of Downstream Slot Area and Slot Configuration

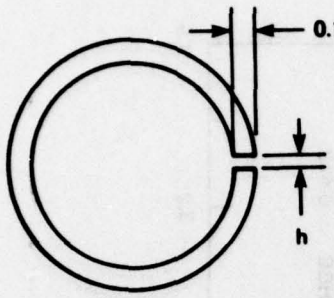

A_s = 0.994 IN.^{2}
h = 0.042 IN.

Figure 13a - Pipe Model

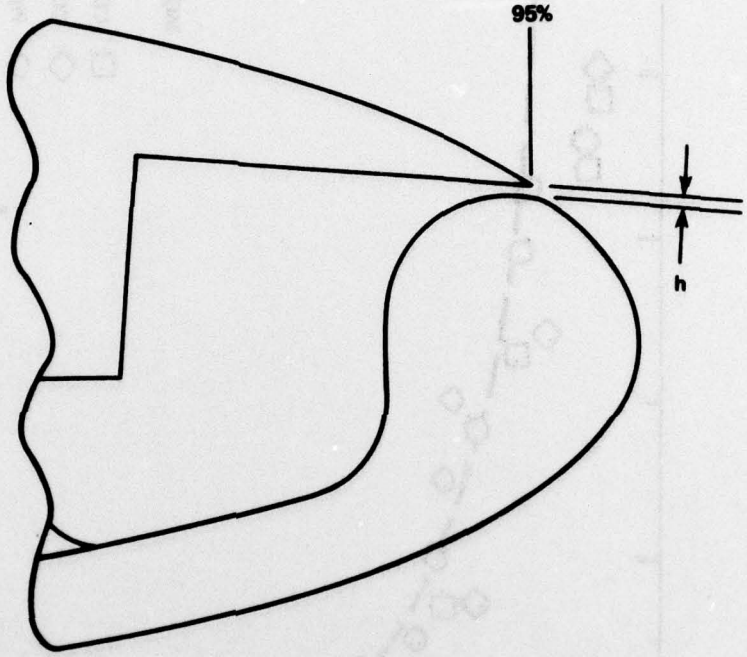

A_s = 0.413 IN.^{2}
h = 0.004 - 0.012 IN.

Figure 13b - HHCC Model

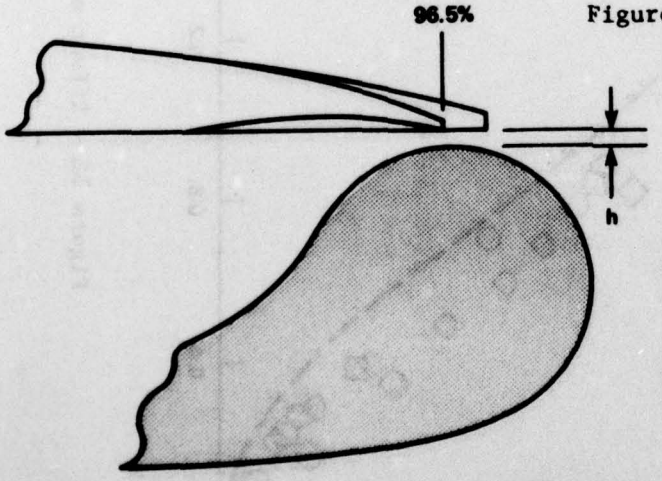

CCR1 – A_s = 0.189 IN.^{2}
h = 0.004 - 0.010 IN.
CCR2 – A_s = 0.199 IN.^{2}
h = 0.004 - 0.010 IN.

Figure 13c - CCR1 and CCR2 Models

Figure 13 - Slot Configurations

Figure 14 - Pressure Loss Coefficient versus Azimuth Position for Various Configurations

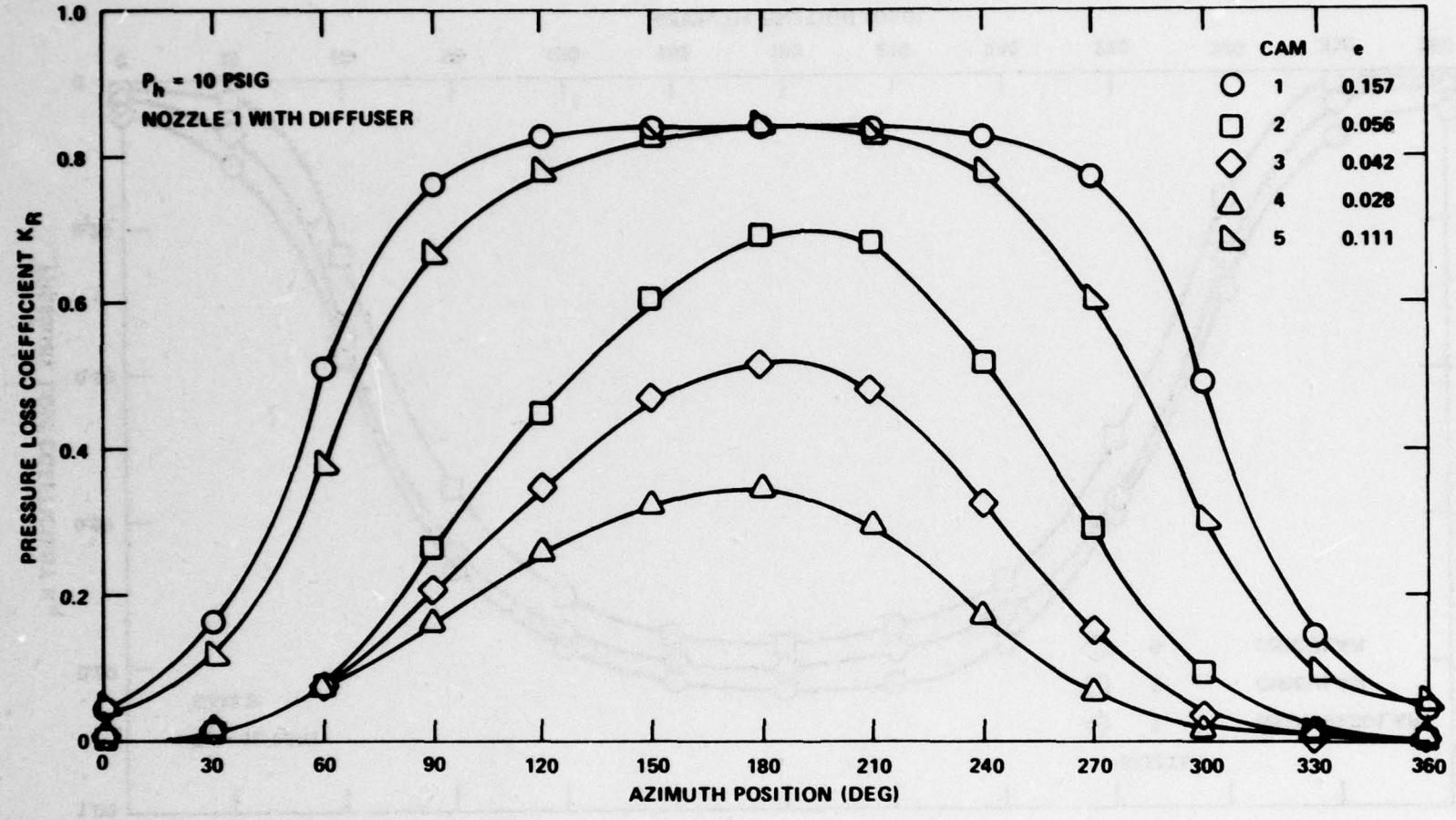

Figure 14a - Various Cams

Figure 14 (Continued)

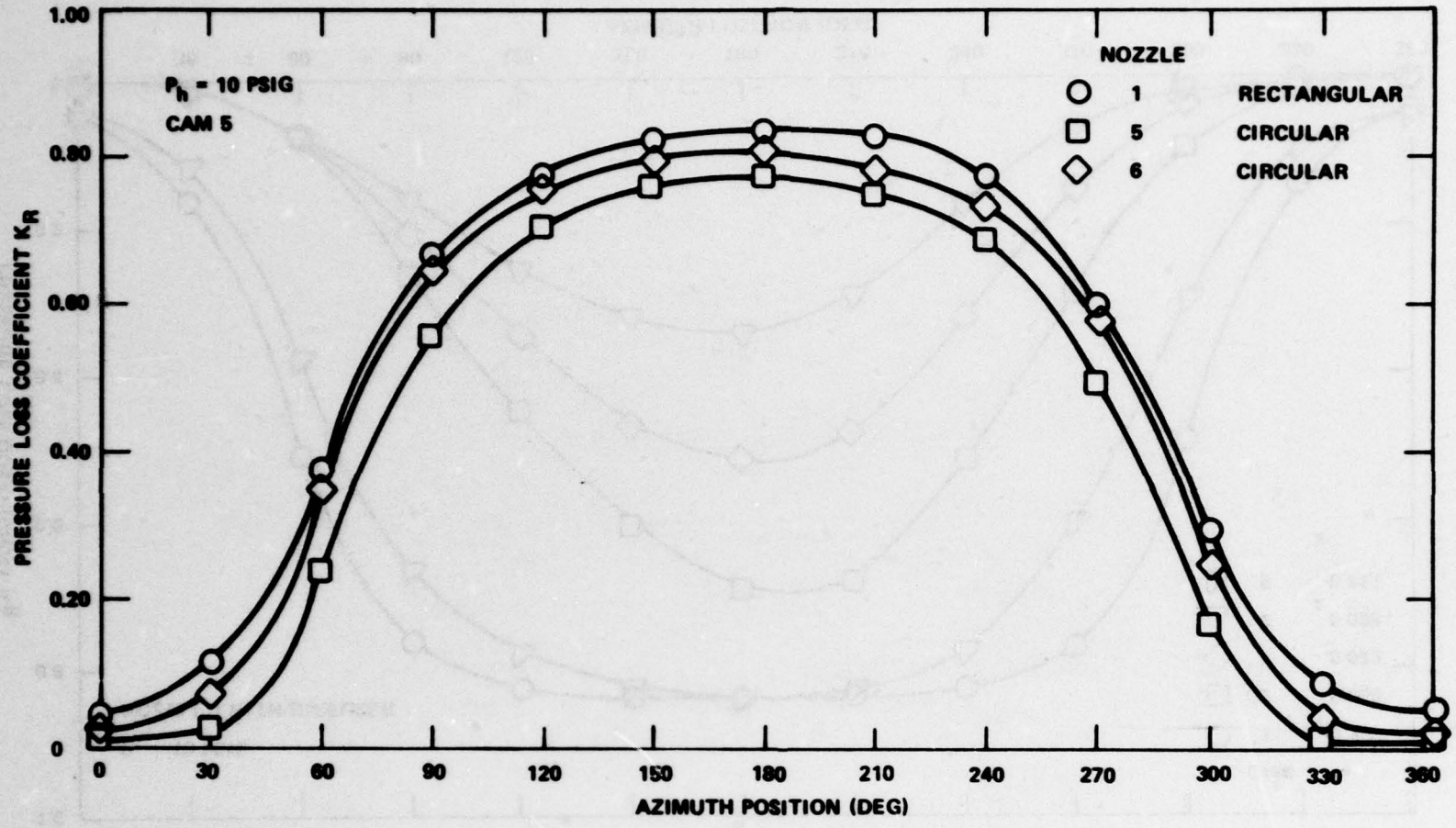

Figure 14b - Nozzles with Contractors

Figure 14 (Continued)

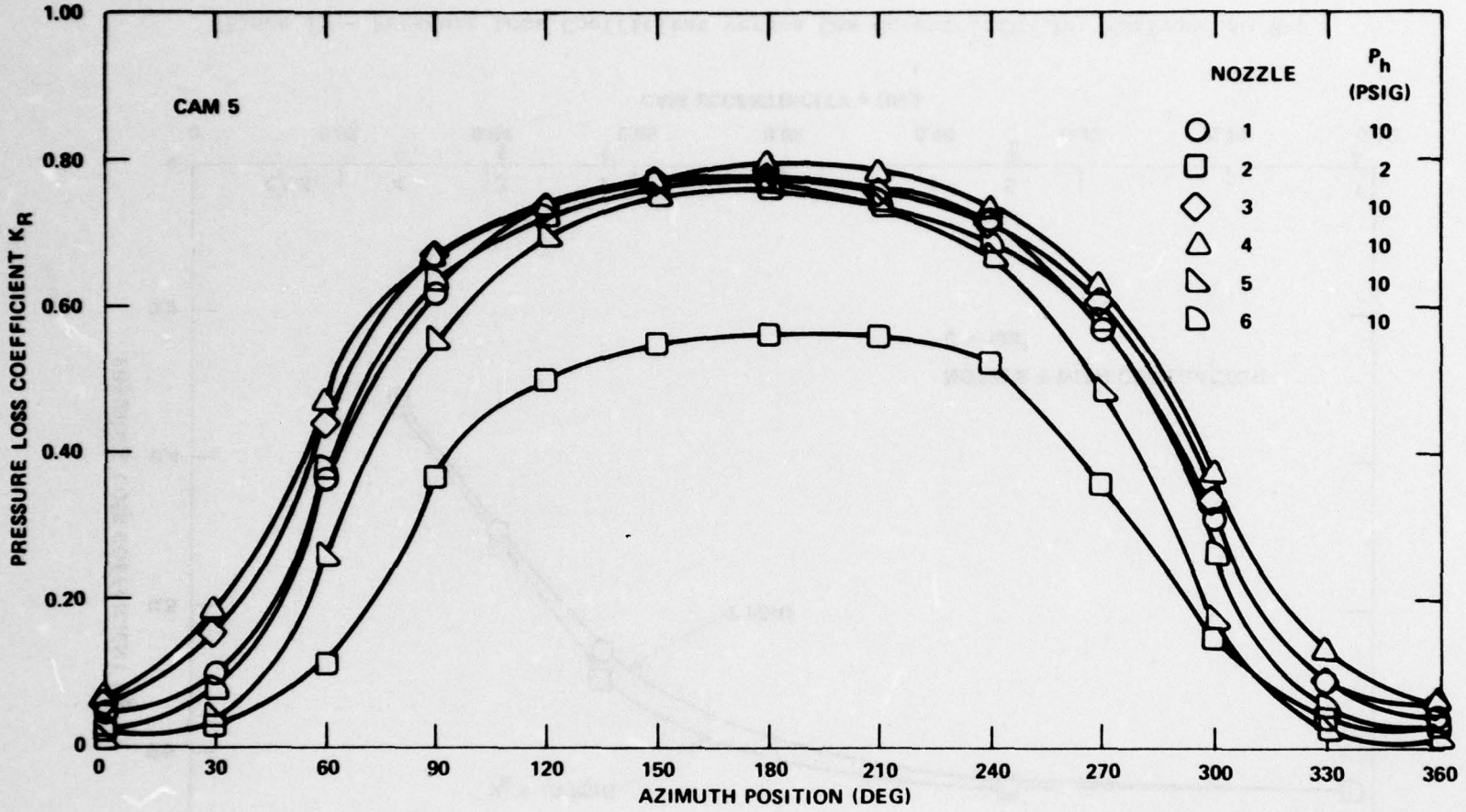

Figure 14c - Nozzles without Contractors

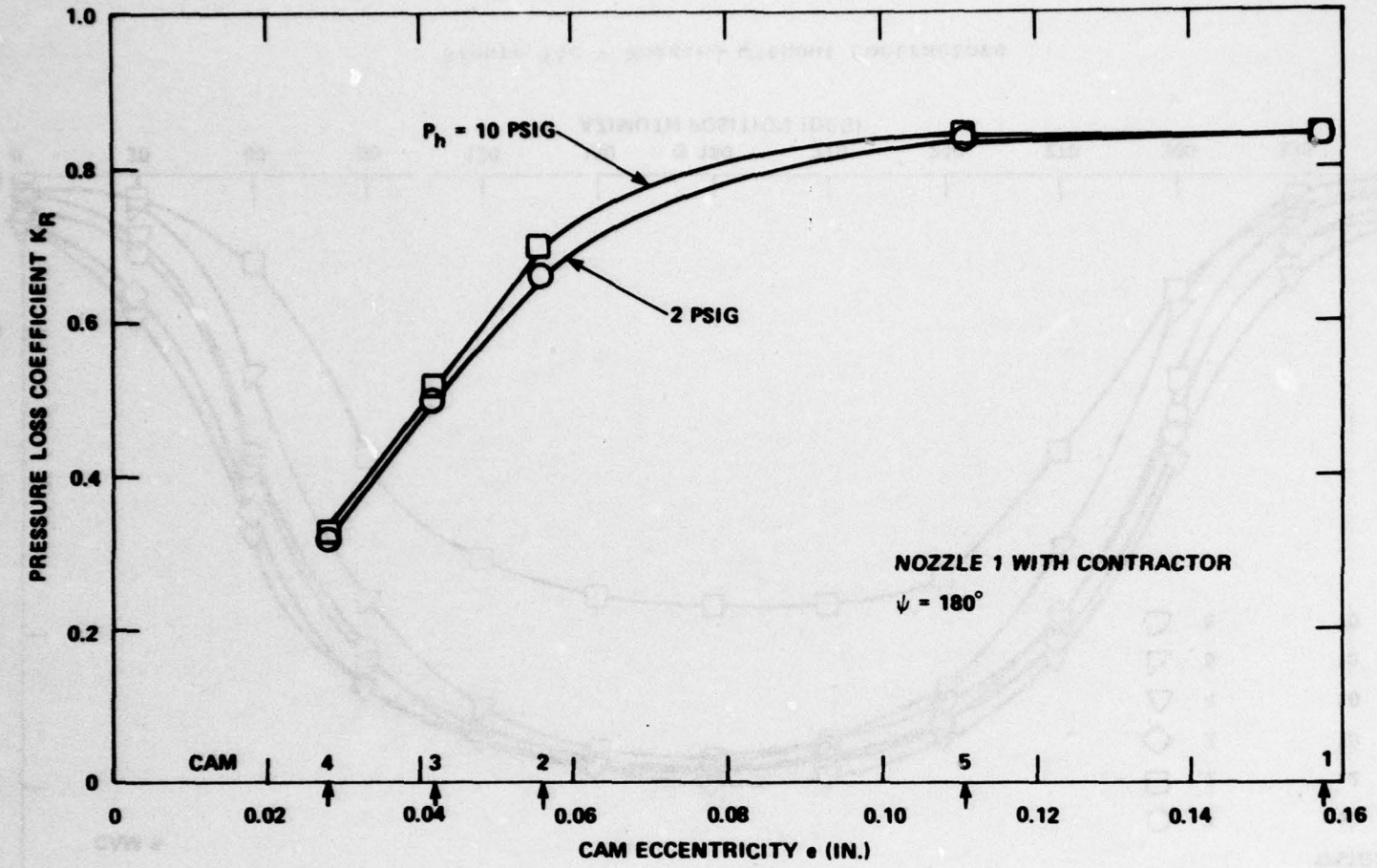

Figure 15 - Pressure Loss Coefficient versus Cam Eccentricity for Maximum Cam Gap

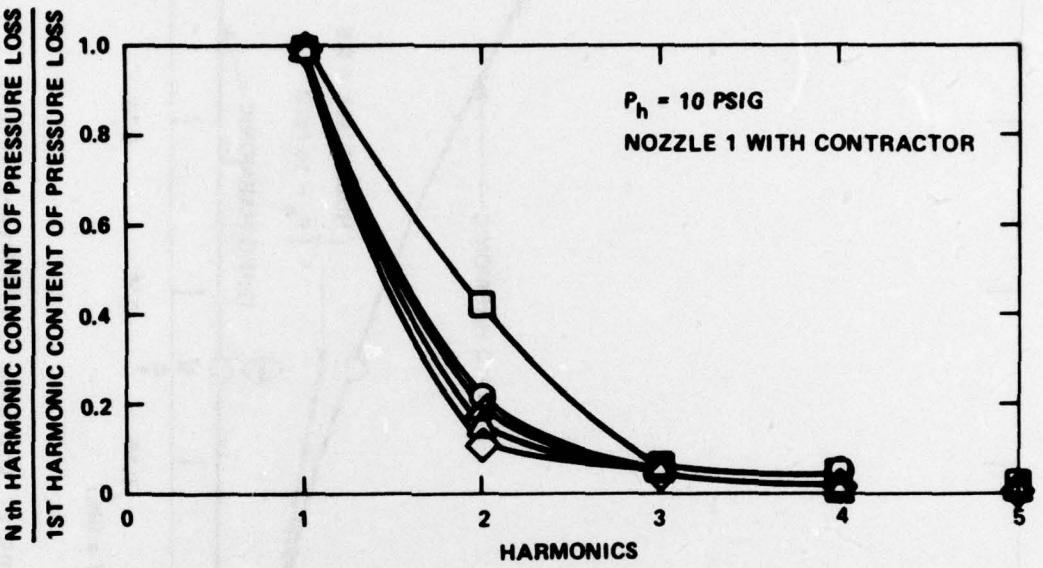

Figure 16a - Harmonic Content of Pressure Loss

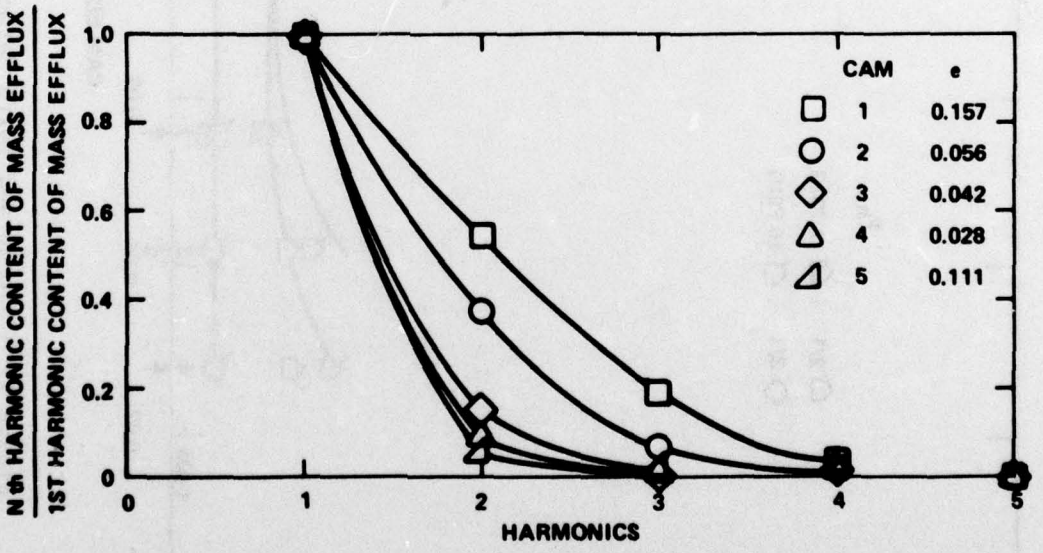

Figure 16b - Harmonic Content of Mass Efflux

Figure 16 - Normalized Harmonic Content for Various Cam Eccentricity

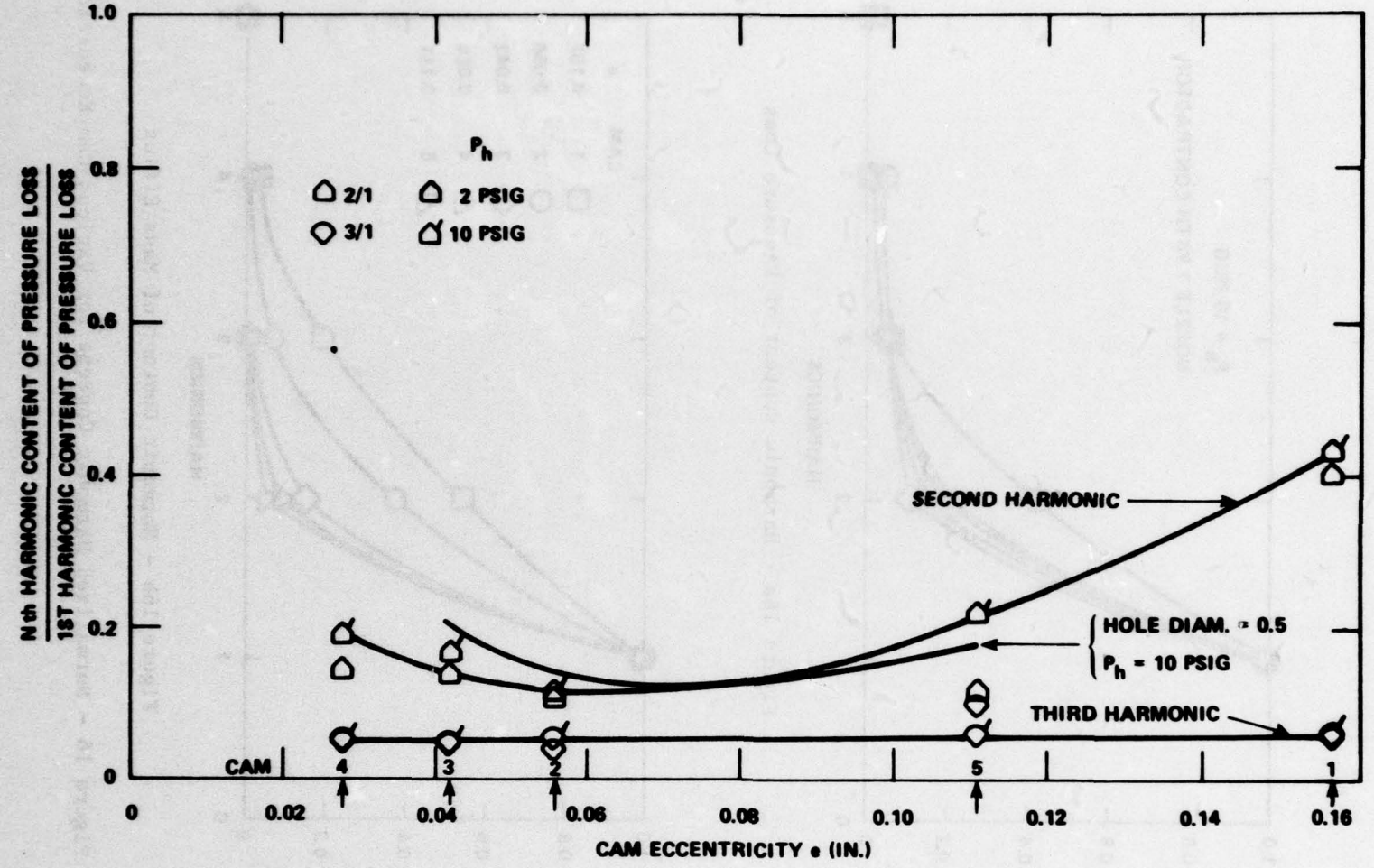

Figure 17 - Second and Third Harmonic Content of the Loss Coefficient versus Cam Eccentricity

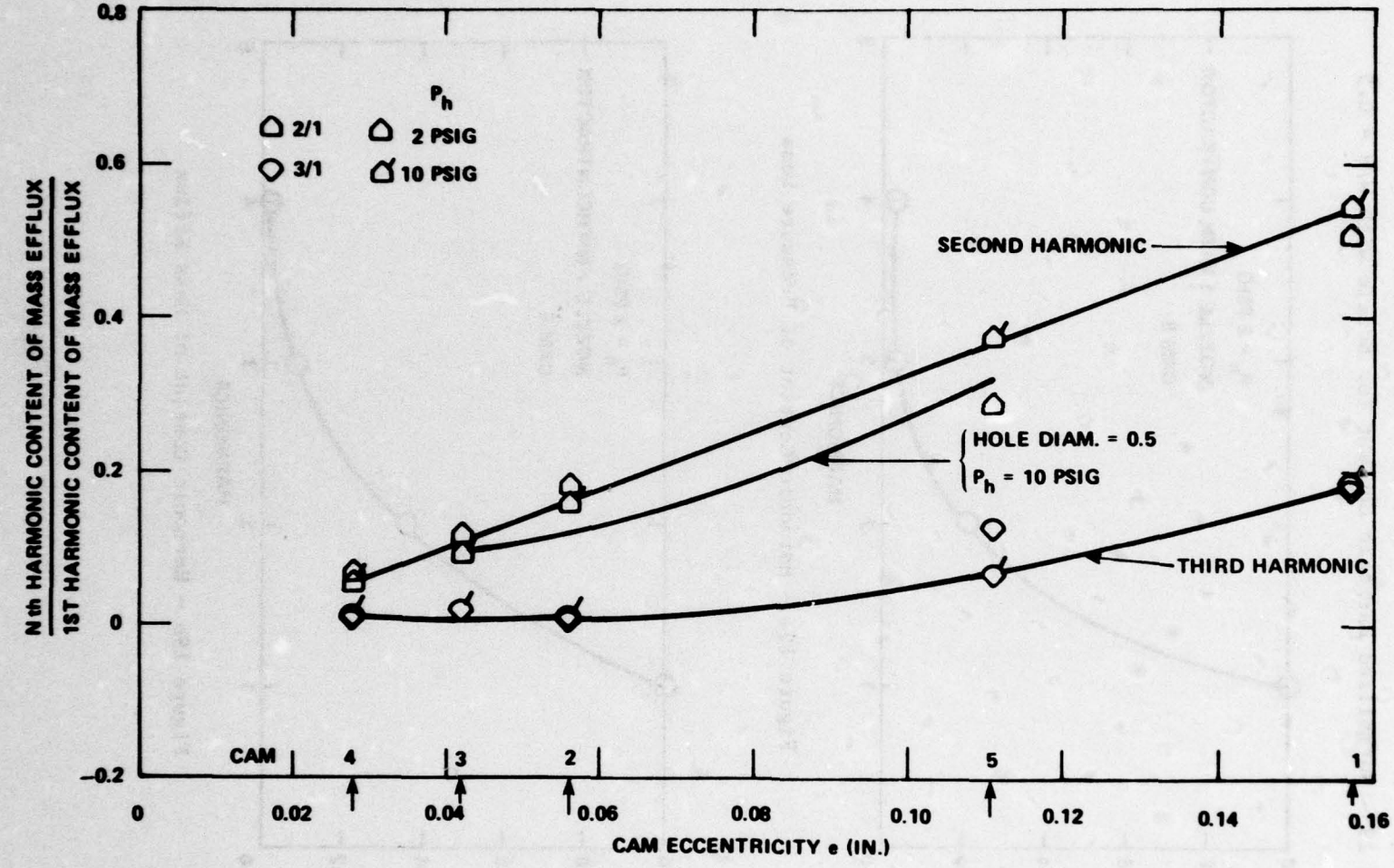

Figure 18 - Second and Third Harmonic Content of Mass Efflux versus Cam Eccentricity

Figure 19 - Normalized Harmonic Content for Nozzle with W/H = 0.5

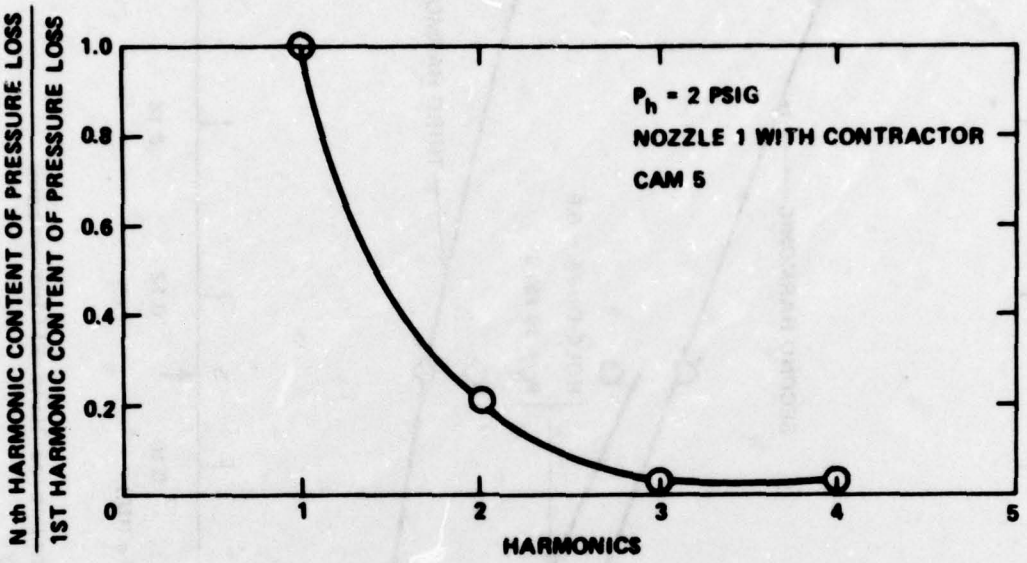

Figure 19a - Harmonic Content of Pressure Loss

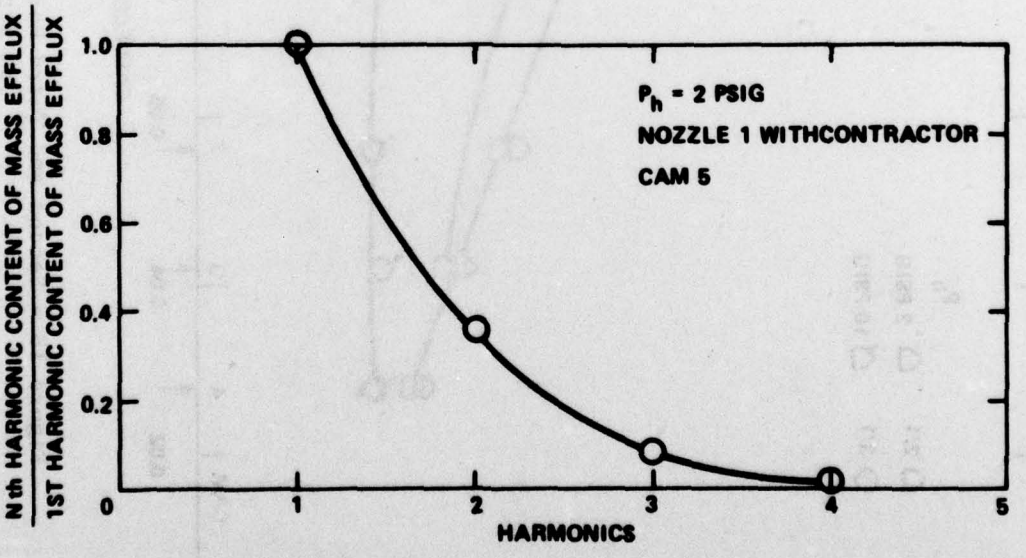

Figure 19b - Harmonic Content of Mass Efflux

Figure 19 (Continued)

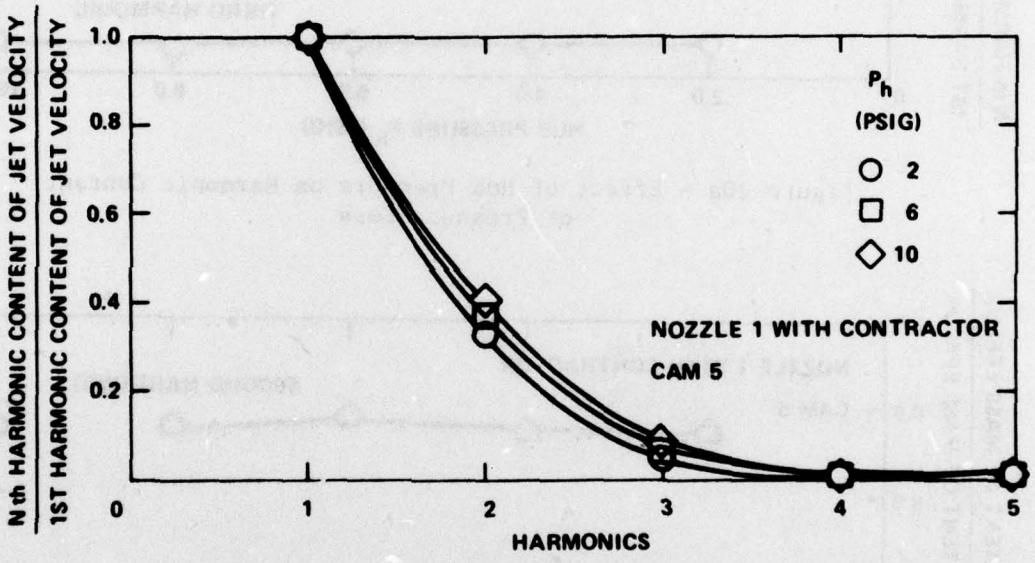

Figure 19c - Harmonic Content of Jet Velocity

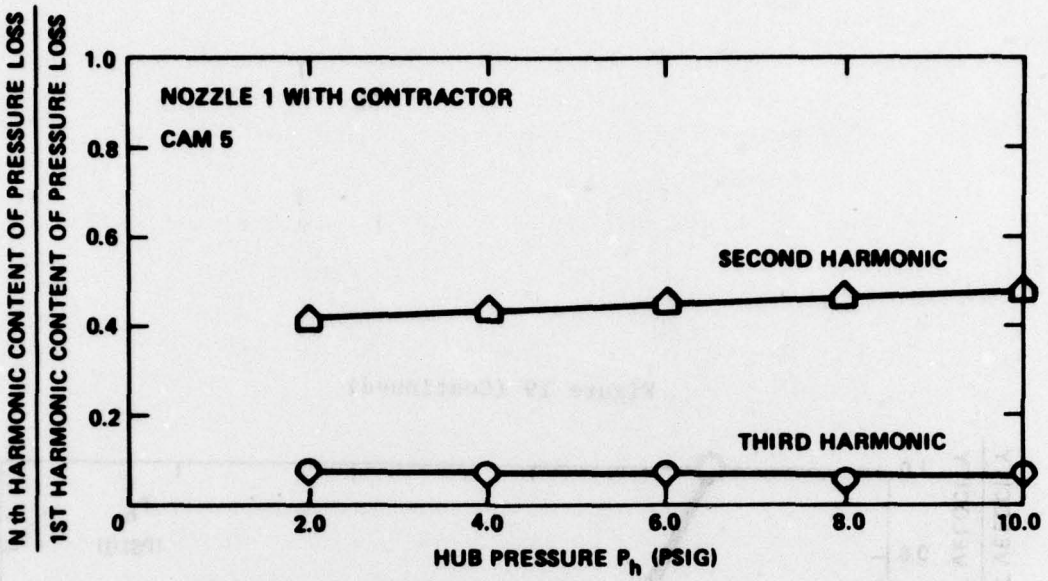

Figure 20a - Effect of Hub Pressure on Harmonic Content of Pressure Loss

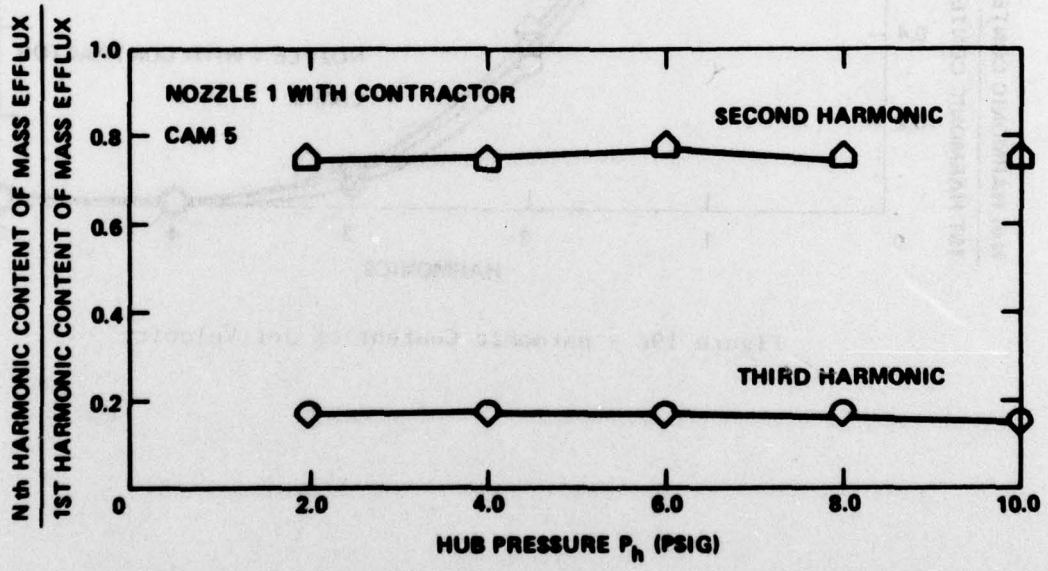

Figure 20b - Effect of Hub Pressure on Harmonic Content of Mass Efflux

Figure 20 - Second and Third Harmonic Content versus Hub Pressure for Nozzle with W/H = 0.5

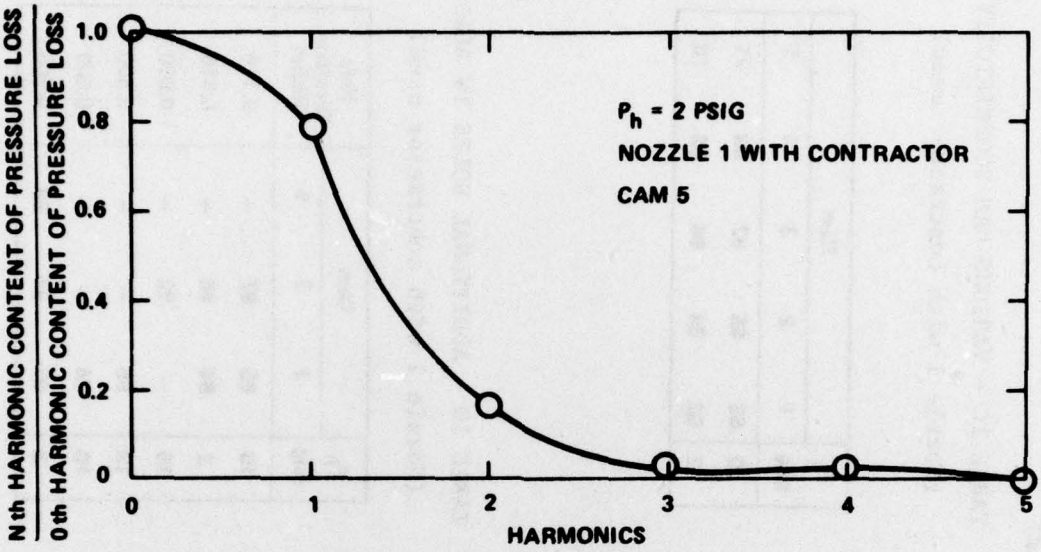

Figure 21a - Harmonic Content of Pressure Loss

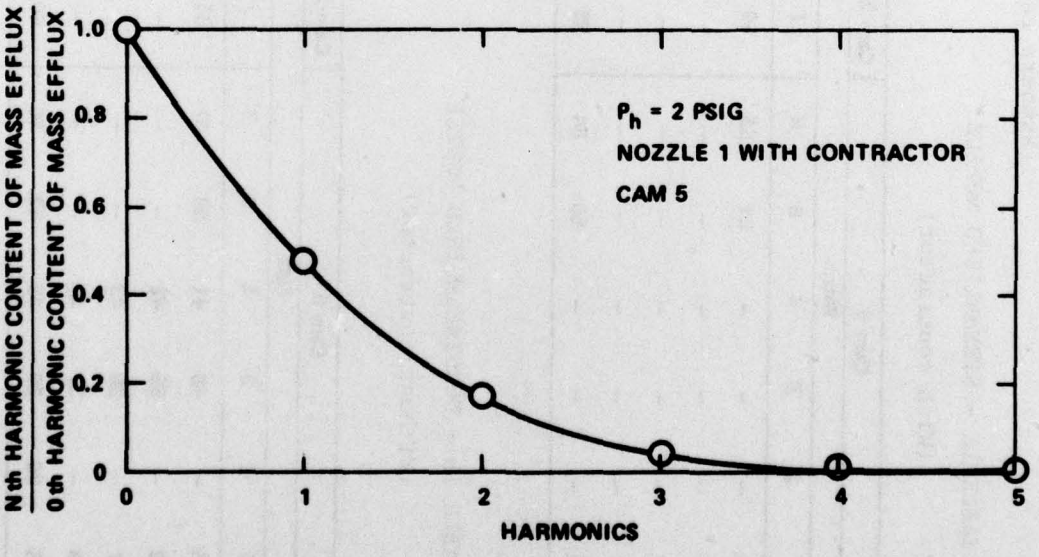

Figure 21b - Harmonic Content of Mass Efflux

Figure 21 - Harmonic Content Normalized by the Constant Term for Nozzle with W/H = 0.5

TABLE 1 - CONFIGURATIONS EVALUATED IN THE TEST PROGRAM

(Numbers refer to runs)

TABLE 1A - STREAMLINED NOZZLE

(With contractor)

P_h psig	Cam 5						Cam 2
	Noz.						
	1	2	3	4	5	6	7
10	5	–	–	–	51	55	59
8	4	–	–	–	–	–	–
6	3	–	–	–	–	–	–
4	2	–	–	–	–	–	–
2	1	–	–	–	50	54	58

TABLE 1B - NONSTREAMLINED NOZZLE

(Without contractor)

P_h psig	Cam 5						Cam 2
	Noz.						
	1	2	3	4	5	6	7
10	29	–	40	41	53	57	61
8	28	–	39	42	–	–	–
6	27	–	38	43	–	–	–
4	26	–	37	44	–	–	–
2	25	30	36	45	52	56	60

TABLE 1C - VARIOUS CAM ECCENTRICITY

(Nozzle 1 with contractor used)

P_h psig	Cam				
	1	2	3	4	5
10	63	65	67	69	71
2	62	64	66	68	70

TABLE 1D - ADDITIONAL HOLES IN BLADE

(Nozzle 1 with contractor used)

P_h psig	Cam			Hole Diameter inches
	2	3	5	
10	85	87	–	0.316
2	84	86	–	0.316
15	–	92	–	0.500
13	95	–	–	0.500
10	94	–	–	0.500
2	93	91	96	0.500